Resumming Signals from Heavy Annihilating Dark Matter

Tracy Slatyer

SCET 2019
UC San Diego
3/27/2019

JHEP 1901 (2019) 036, PRD98 123014 (2018), and JHEP 1803 (2018) 117, with M. Baumgart, T. Cohen, E. Moulin, I. Moult, L. Rinchiuso, N. Rodd, M. Solon, I. Stewart and V. Vaidya

Outline

- Review of dark matter and heavy WIMPs
- The wino / SU(2) triplet as a dark matter model + illustrative case for general dark sectors
  - Collider/direct constraints (and lack thereof) + the power of indirect detection
  - Importance of resummation for annihilation signals
  - Interplay with nonrelativistic potential effects
- The hard gamma-ray spectrum from wino annihilation
  - Mode structure
  - Two-stage factorization
  - NLL precision spectrum results
- Forecasts for sensitivity of current/future DM searches in gamma rays

What is dark matter?

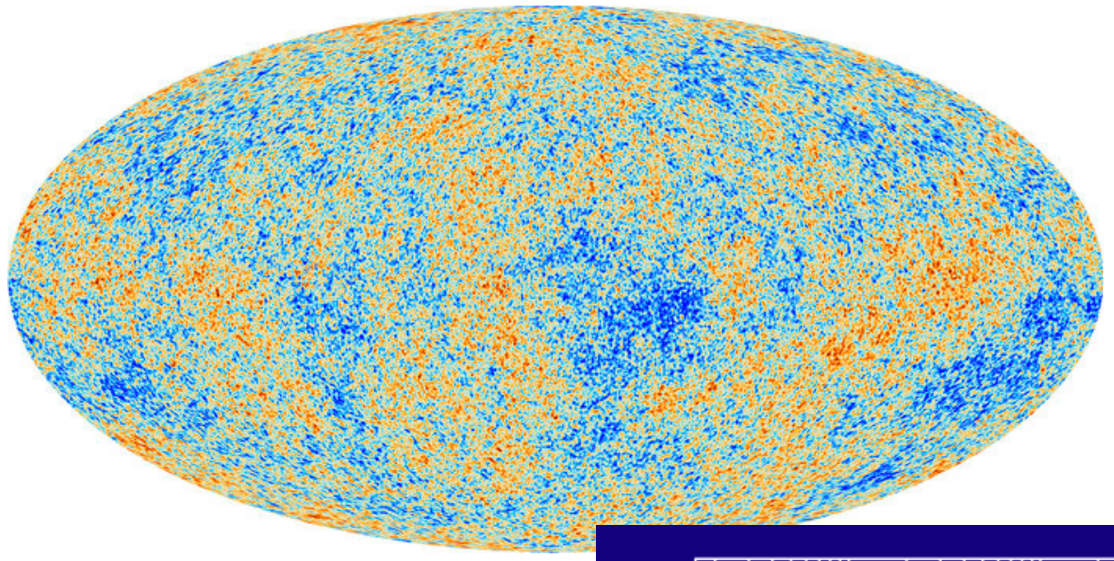

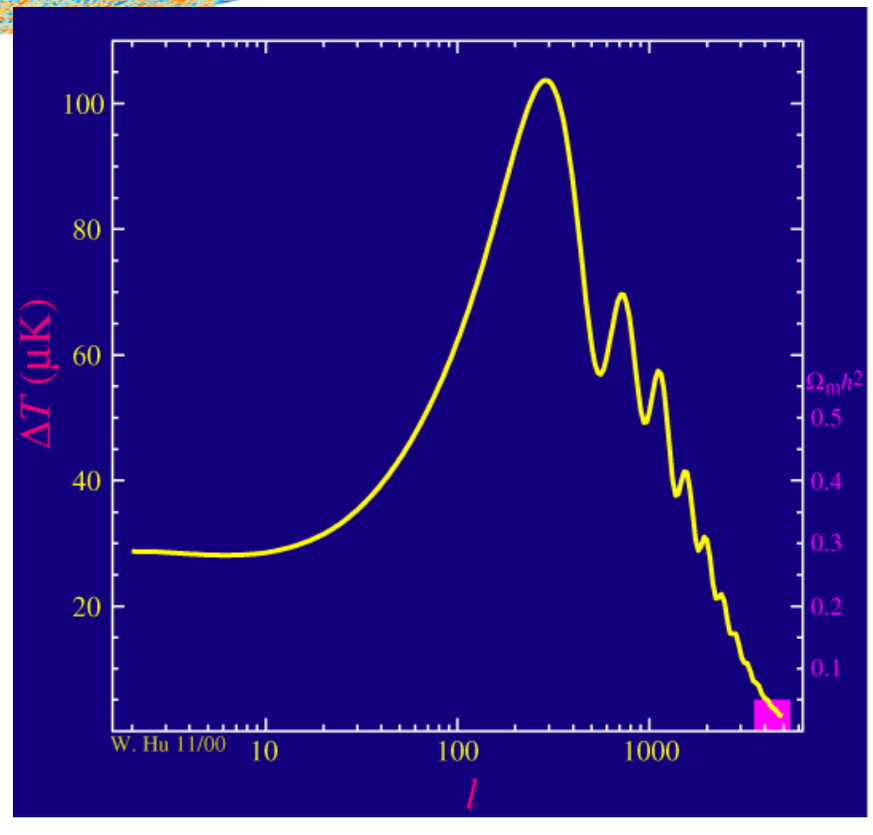

We know it:

- Is roughly 80% of the matter in the universe.
- Gravitates / has mass.
- Doesn't scatter/emit/absorb light (really "transparent matter"!)
- Interacts weakly or not at all (except by gravity).
- Isn't made up of any known particles.

Wayne Hu, http://background.uchicago.edu/~whu/

What is dark matter?

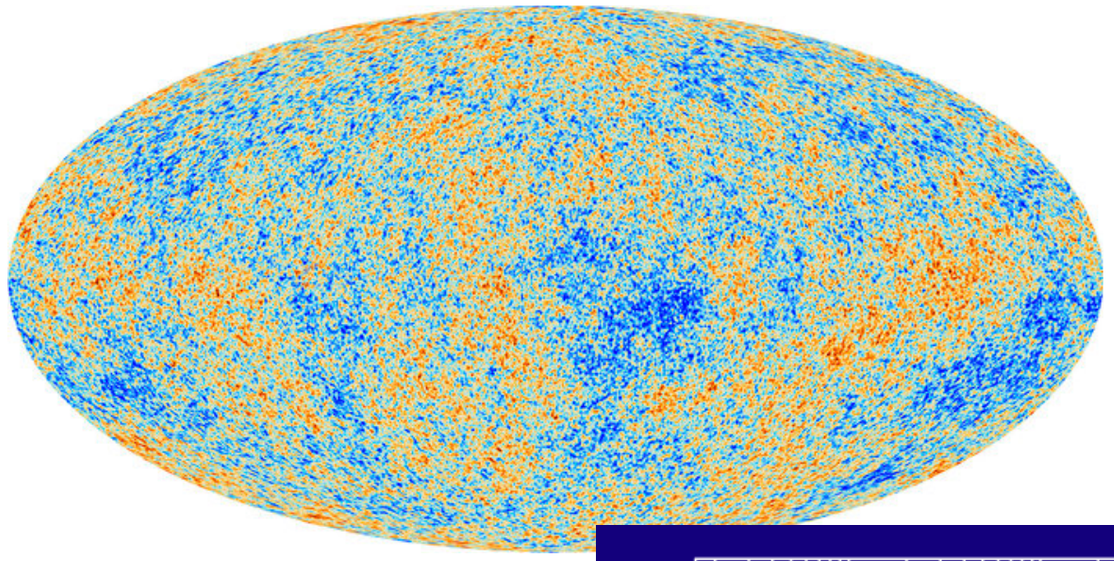

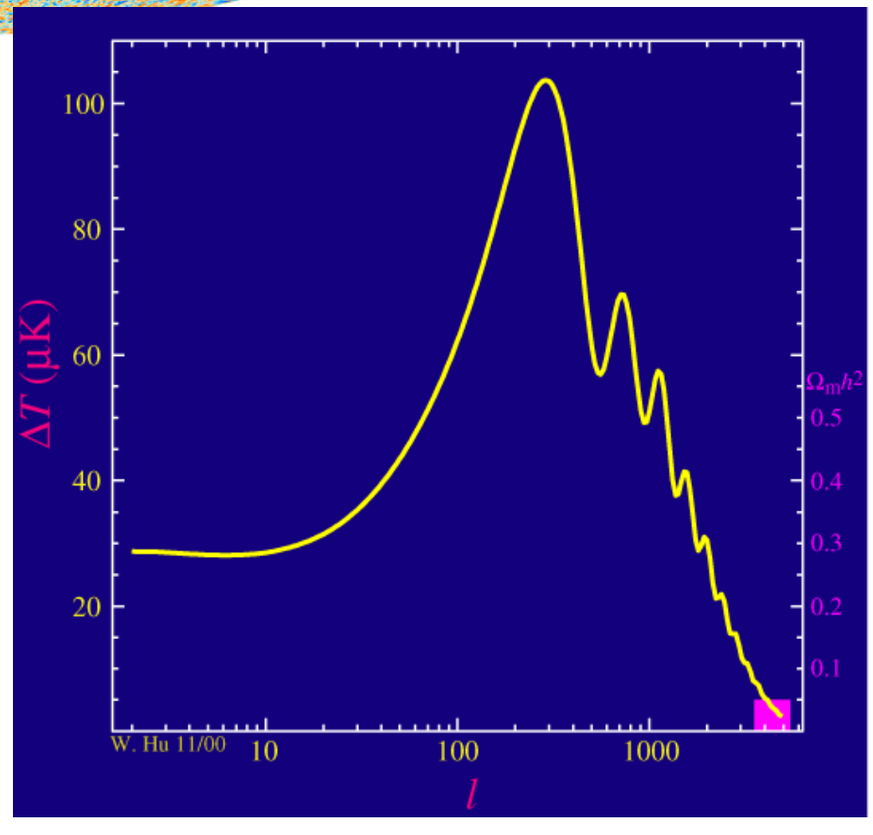

We know it:

- Is roughly 80% of the matter in the universe.
- Gravitates / has mass.
- Doesn't scatter/emit/absorb light (really "transparent matter"!)
- Interacts weakly or not at all (except by gravity).
- Isn't made up of any known particles.

Wayne Hu, http://background.uchicago.edu/~whu/

What is dark matter?

<u>We know it:</u>

- Is roughly 80% of the matter in the universe.
- Gravitates / has mass.
- Doesn’t scatter/emit/absorb light (really “transparent matter”!)
- Interacts weakly or not at all (except by gravity).
- Isn’t made up of any known particles.

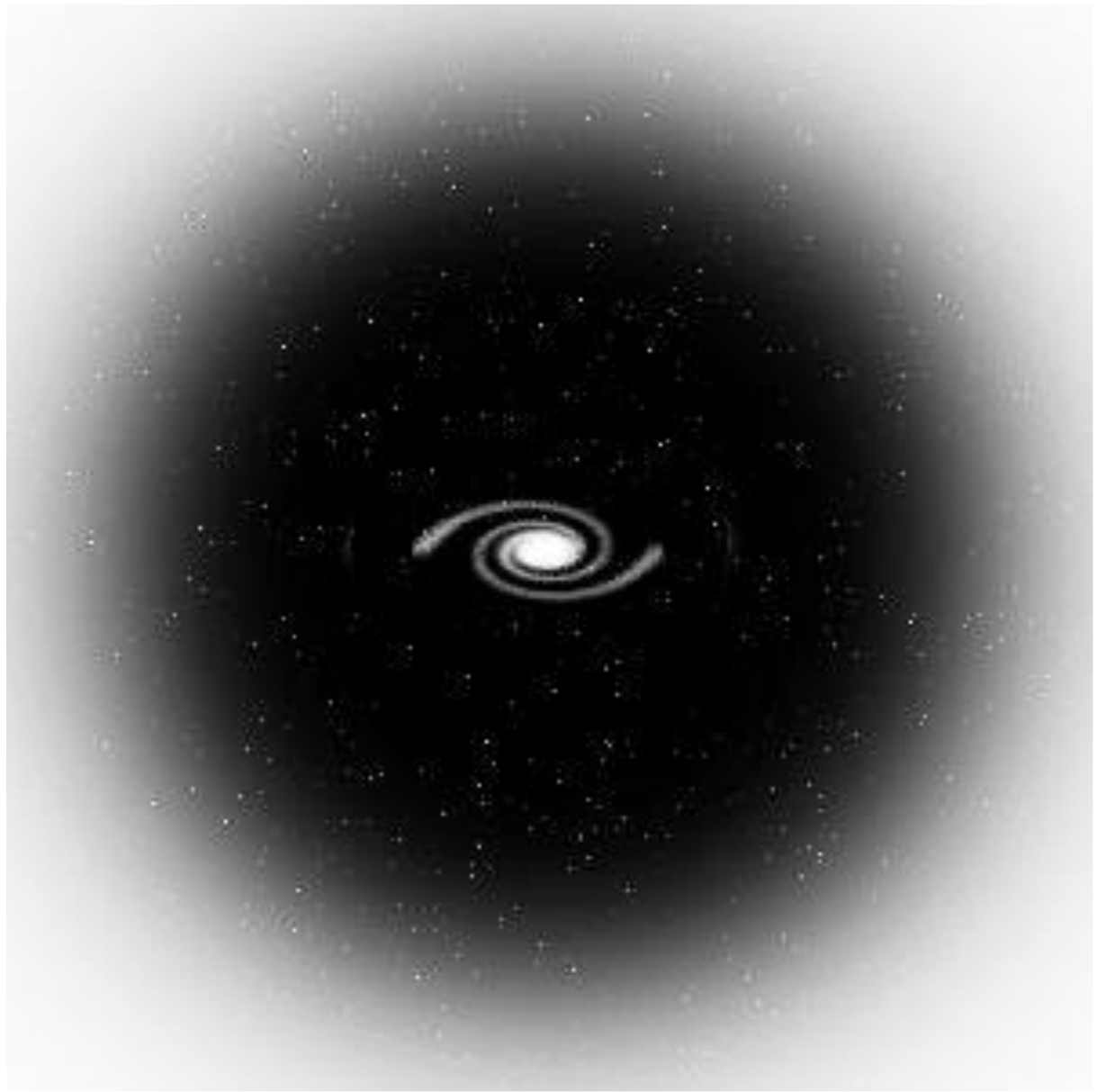

What is dark matter?

We know it:

- Is roughly 80% of the matter in the universe.
- Gravitates / has mass.
- Doesn’t scatter/emit/absorb light (really “transparent matter”!)
- Interacts weakly or not at all (except by gravity).
- Isn’t made up of any known particles.

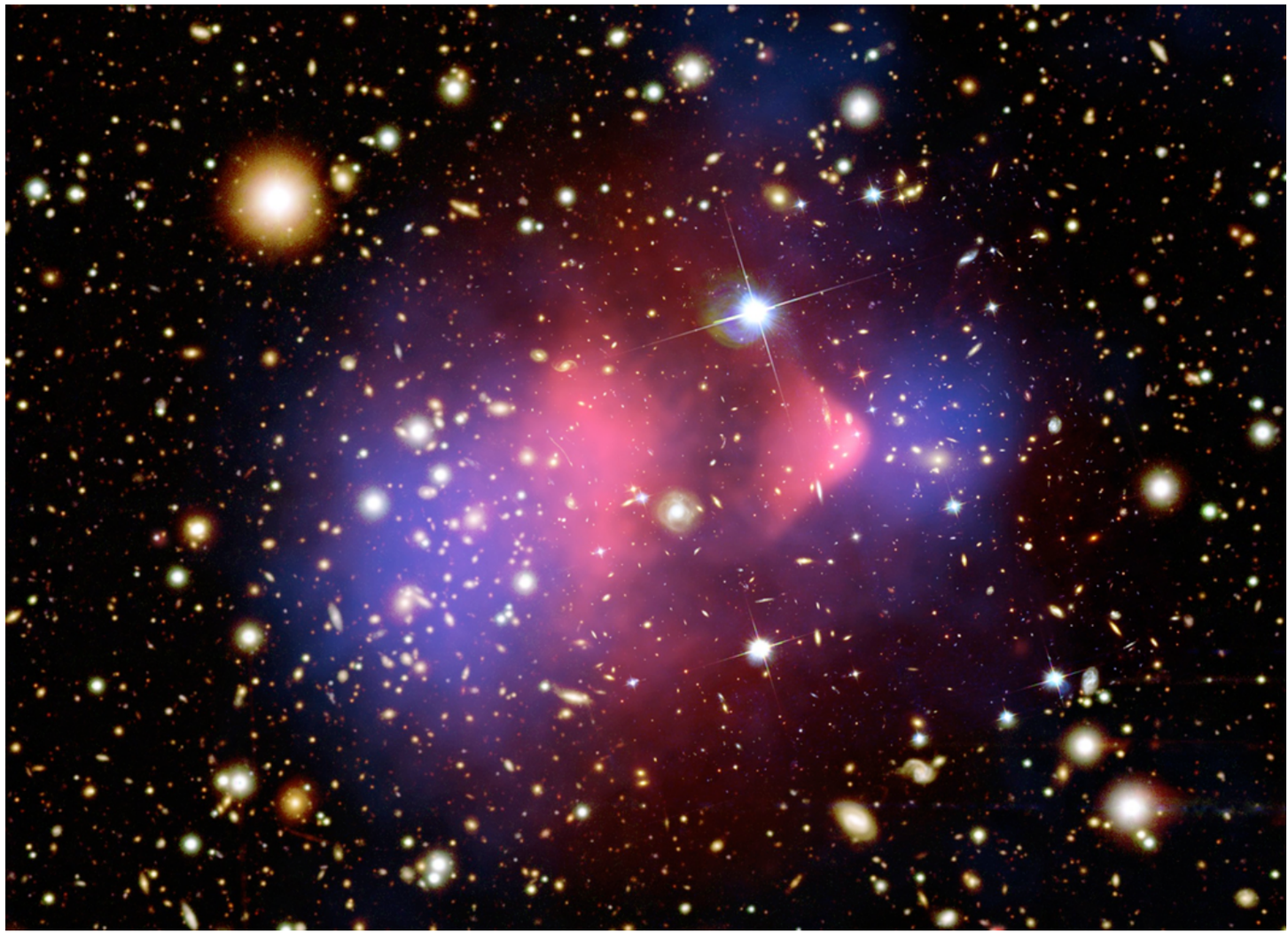

The case for WIMPs

- There is an enormous range of possible mass scales for particle DM, from ~10^{-22} eV up to the Planck scale.

- One possible scenario: annihilation reactions deplete DM in the early universe, control its present-day abundance.

- In this “thermal freezeout” scenario, DM must have a mass between ~1 MeV and 100 TeV (in standard cosmology).

- Required annihilation cross section is ~$1/(100\ \mathrm{TeV})^2 \sim \alpha^2/\mathrm{TeV}^2$ - consistent with weak-scale mass and interaction strength.

- Motivates DM as a Weakly Interacting Massive Particle (WIMP).

Are WIMPs ruled out?

- The GeV-TeV mass range most strongly motivated by this argument has been studied extensively (& lots of recent+ongoing work on the sub-GeV range).
- No detection (yet) of new weak-scale physics at the LHC.
- No detection (yet) of WIMPs in direct or indirect dark matter searches - direct searches probing cross sections as small as 4×10^{-47} cm^2 (XENON1T Collaboration '18).
- Can we exclude thermal relic dark matter where:
  - The DM transforms under the gauge groups of the Standard Model, or
  - The DM simply has roughly weak-scale masses and couplings?
- Classic example: dark matter as the Lightest Supersymmetric Particle (LSP), stabilized by R-parity. Typically the LSP is the lightest neutralino - admixture of bino, wino and higgsino (superpartners of gauge + Higgs bosons).

The wino

- Fermionic dark matter in triplet representation of $SU(2)_L$.
- After electroweak symmetry breaking, consists of Majorana neutralino χ^0 and slightly heavier Dirac chargino $\chi^+\chi^-$.
- Appears in supersymmetric theories as the superpartner of the W boson.
- I will focus on the limit where the wino is the lightest supersymmetric particle and mixing with the other neutralinos is small ("pure wino").

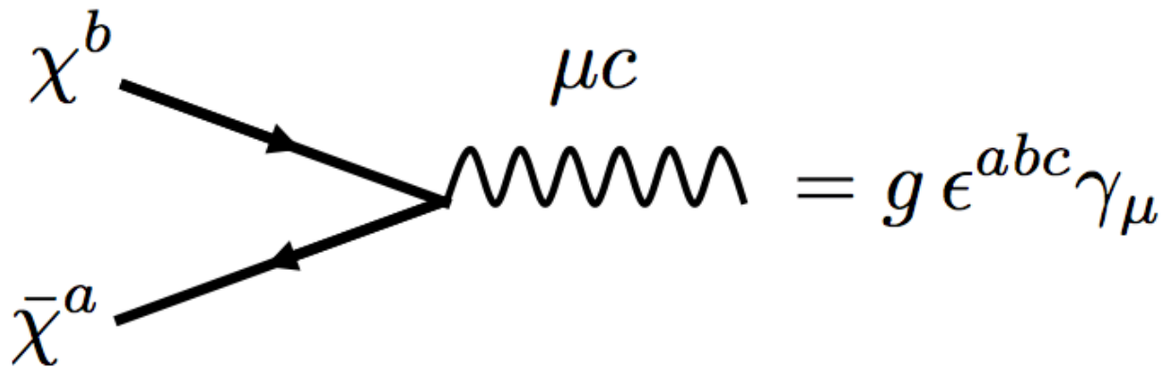

Spectrum/interactions after symmetry breaking:

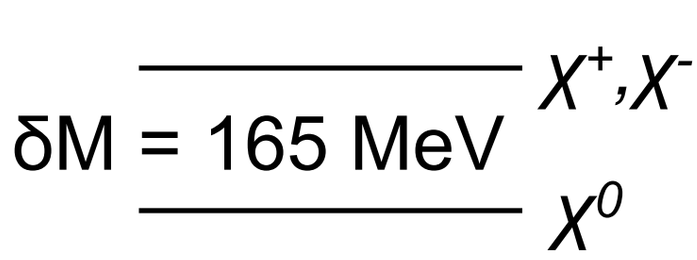

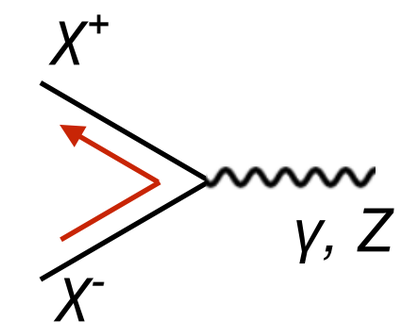

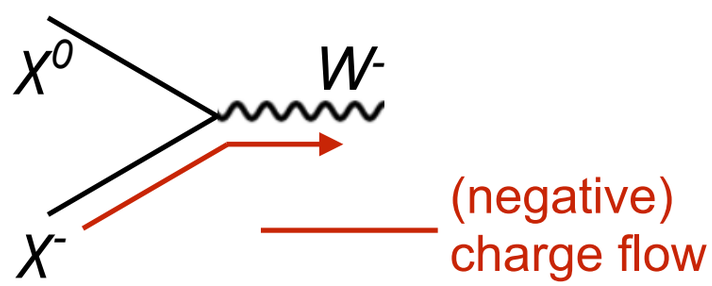

Abundance and mass scale

- Abundance is determined through “thermal freezeout” mechanism, primarily by annihilation to W bosons.

- Yields the correct thermal relic abundance with mass ~3 TeV for the pure wino, with a broader range for admixed winos [Beneke et al ’16].

- At lower masses would constitute a subdominant DM component.

- Collider searches for disappearing chargino tracks only restrict mass to be > 400 GeV.

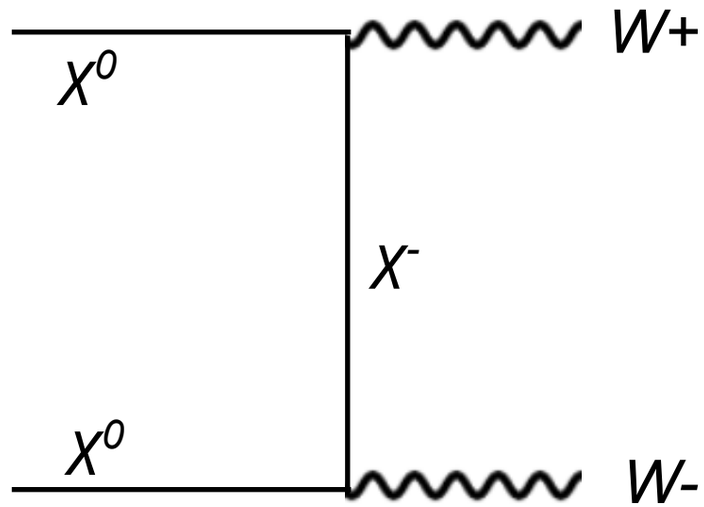

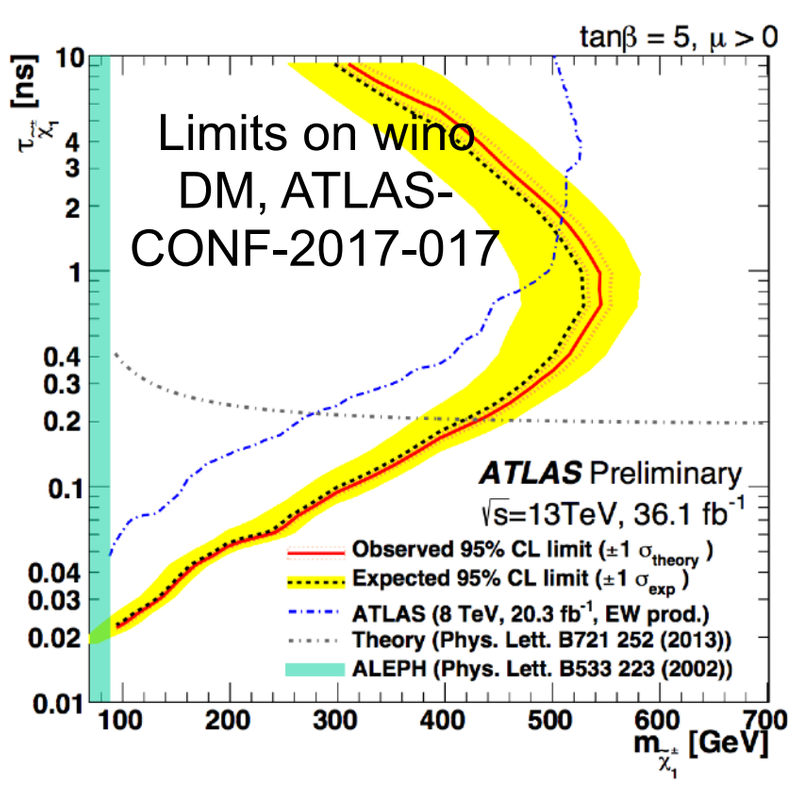

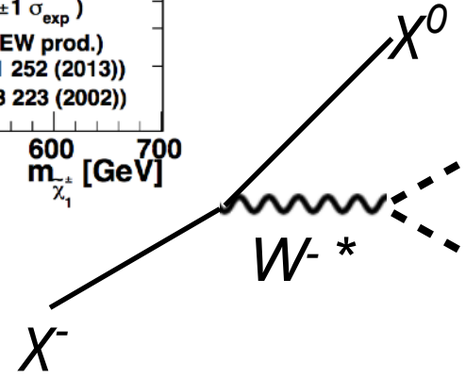

Searching for the heavy wino

- This follows general pattern for SUSY WIMPs - LHC constrains sub-TeV region, but at ~TeV+ masses, need other probes.

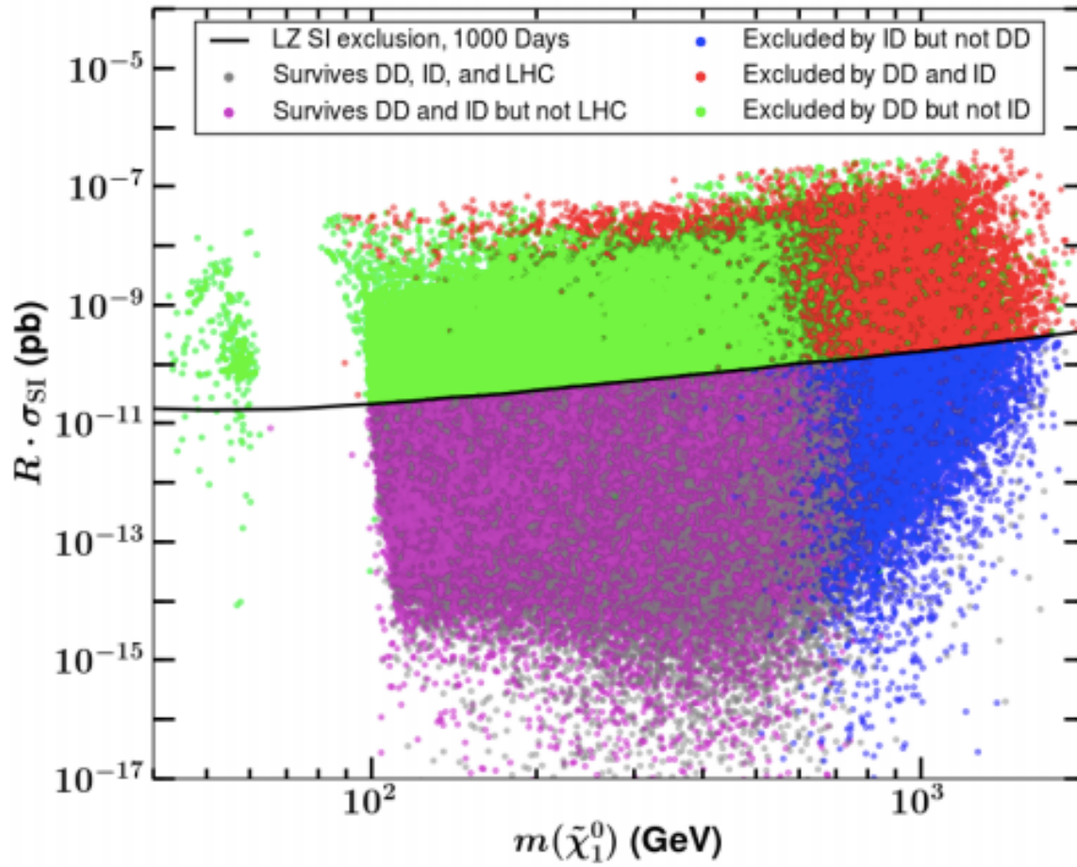

Cahill-Rowley et al '14

- What about direct detection?

- Wino couples to nuclei through W loop (and cross section also suffers destructive interference) - expected signal is very small.

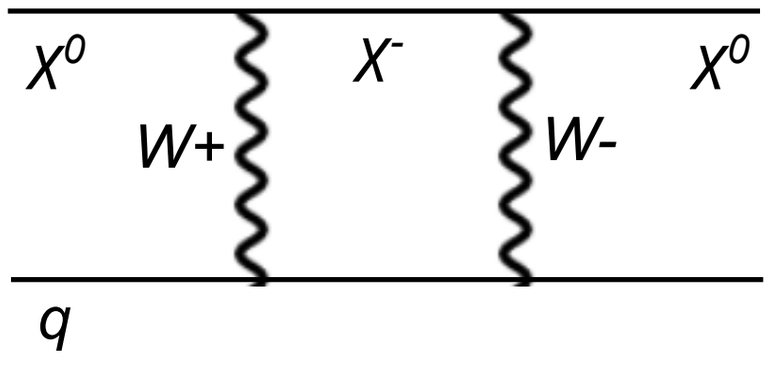

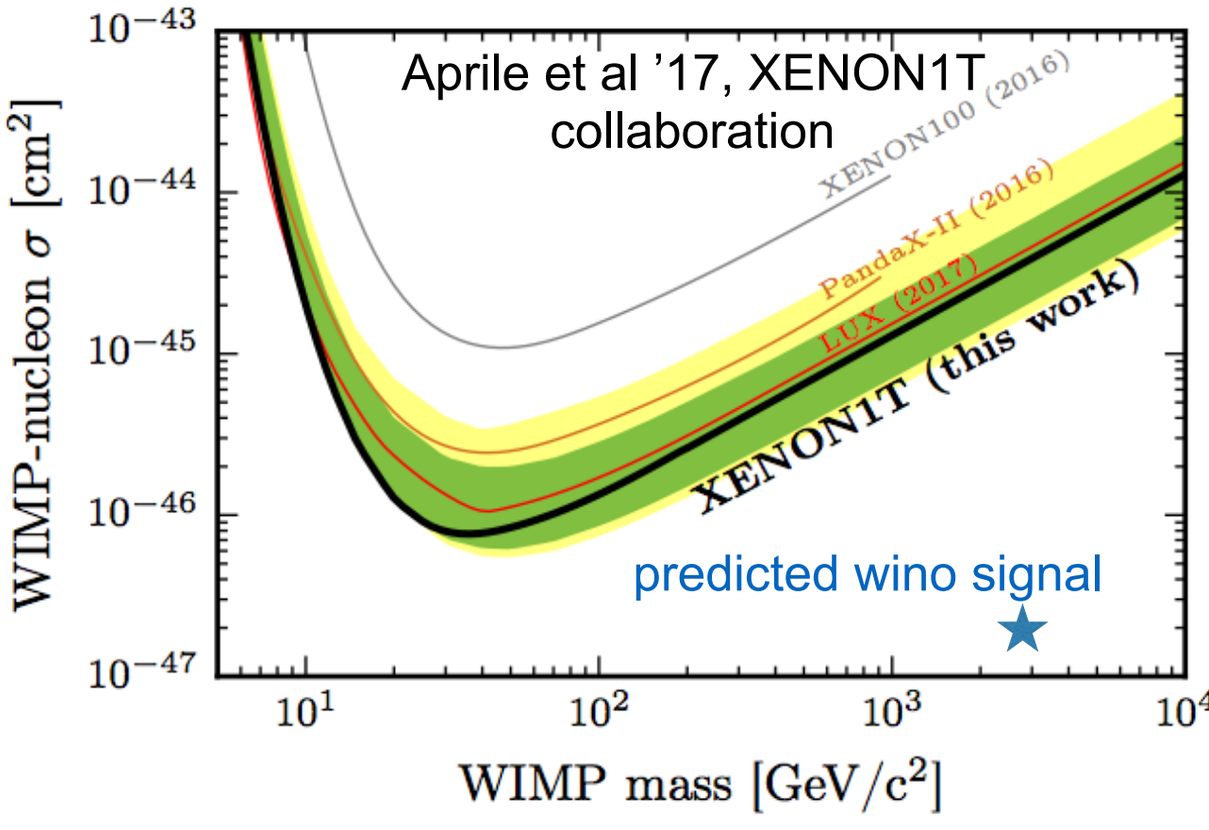

*Hill & Solon '14

The (thermal) wino as a toy model

- Interesting scenario in its own right - simple, predictive, naturally invisible to direct/collider searches.

- Hard to see how we claim to exclude WIMPs if we can't exclude the thermal wino+higgsino.

- But also, because of high DM mass relative to W/Z bosons, electroweak interaction behaves like a long-range force.

- Understanding wino physics thus serves as an illustration of more general scenarios with new "dark sector" force carriers, much lighter than the DM.

Light dark forces

- Simplest scenario: one new “dark force”, carried by a “dark photon” which mixes with the regular photon (+ possibly a second force mediated by a dark Higgs-like boson)

- Every Standard Model particle acquires a tiny “dark charge” - Standard Model processes can (rarely) produce dark photons [for a review of different searches, see U.S. Cosmic Visions Community Report: arXiv 1707.04591]
  - Can be searched for at accelerators (e.g. APEX, Heavy Photon Search, DarkLight)

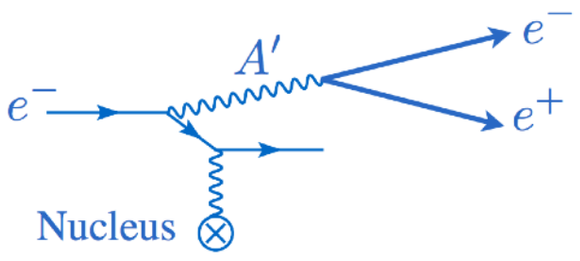

  - Could modify the cooling of supernovae

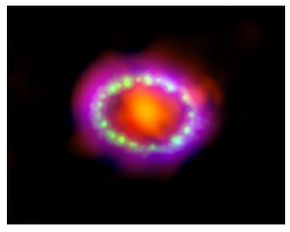

  - Dark matter self-interactions could have observable effects on the dark matter distribution - e.g. changing the densities of galaxies

- More complex scenarios are also viable - the dark sector could have multiple force carriers, like the gauge bosons of the Standard Model

Consequences of a large mass hierarchy

1. Sommerfeld enhancement - long-range attractive potential enhances annihilation processes

2. Bound states - formation of bound states + subsequent decay acts as a new annihilation channel

3. Large logs from small force carrier masses - big radiative corrections to annihilation rate/spectrum, need to be resummed.

Consequences of a large mass hierarchy

1. Sommerfeld enhancement - long-range attractive potential enhances annihilation processes

2. Bound states - formation of bound states + subsequent decay acts as a new annihilation channel

3. Large logs from small force carrier masses - big radiative corrections to annihilation rate/spectrum, need to be resummed.

Can be efficiently calculated with SCET methods

Consequences of a large mass hierarchy

1. Sommerfeld enhancement - long-range attractive potential enhances annihilation processes can be factorized from short-range physics
2. Bound states - formation of bound states + subsequent decay acts as a new annihilation channel
3. Large logs from small force carrier masses - big radiative corrections to annihilation rate/spectrum, need to be resummed.

Can be efficiently calculated with SCET methods

Gamma-ray (line) searches

- Air/water Cherenkov telescopes can probe gamma rays in the 100 GeV - 100 TeV range.
- Gamma-ray line signal from $\chi\chi \to \gamma\gamma$ or $\chi\chi \to \gamma Z$ is a very "clean" possible annihilation channel - no astrophysical lines expected.
- Best prospect for a "smoking gun" indirect signal for DM.
- Stringent constraints from Fermi-LAT at sub-TeV energies, H.E.S.S telescope at TeV+ energies.
- However, branching ratio is typically expected to be small, as DM is dark - no direct coupling to photons.

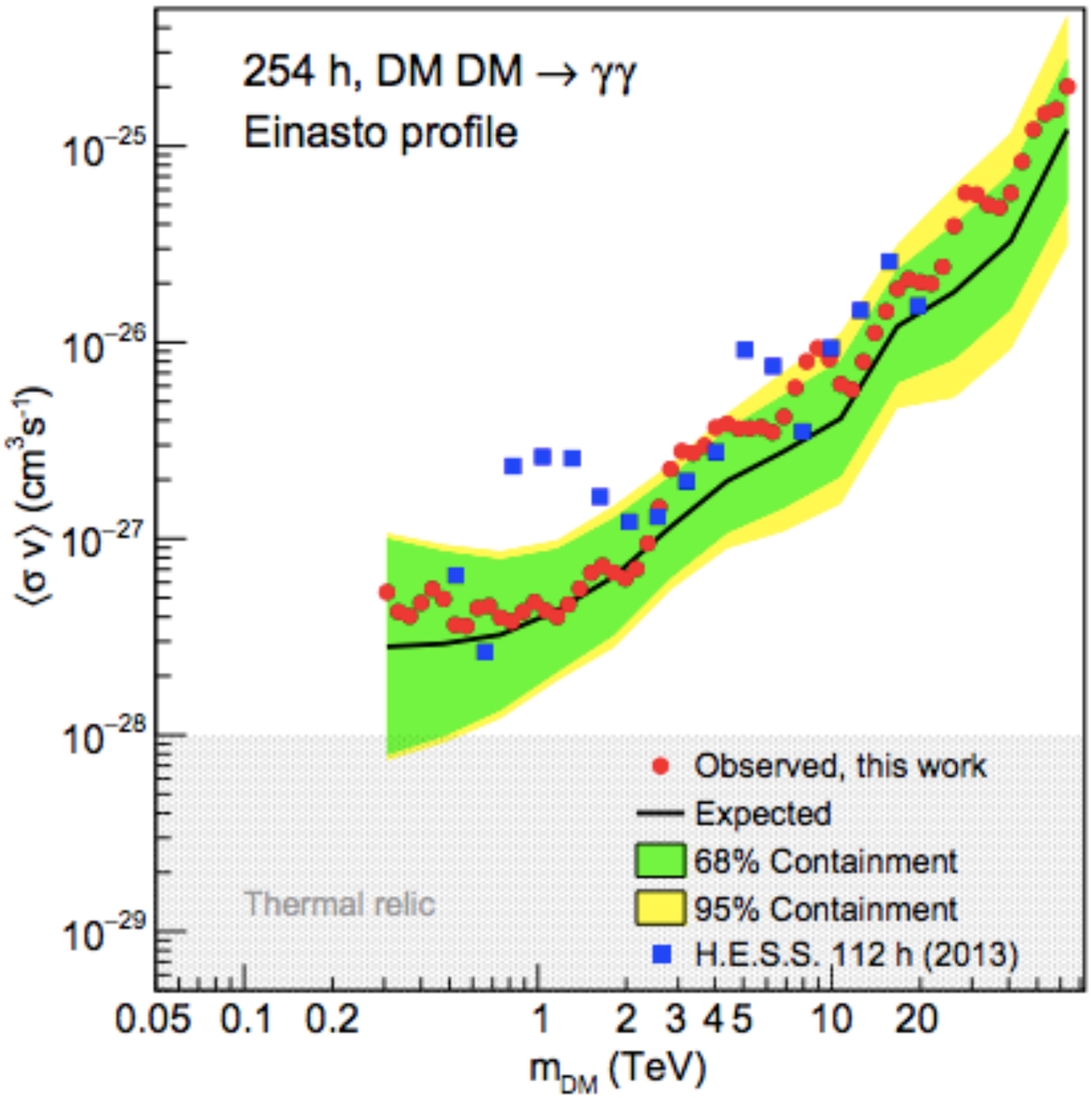

H.E.S.S. Collaboration '18 (1805.05741)

Winos are great at making gamma-ray lines!

- Naive expectation: DM doesn't couple directly to photons, so line signal will be loop suppressed and small.

- This expectation breaks down for winos when DM mass $m_\chi > m_W/\alpha_W$.

- Long-range potential from W exchange allows virtual excitation from $\chi^0\chi^0$ to (nearly degenerate) $\chi^+\chi^-$ state. Can annihilate at tree-level to $\gamma\gamma$, γZ, ZZ.

- General lesson: the long-range potential can affect <u>relative</u> detectability of different channels, e.g. enhancing line signals if particles in the ladder diagrams are charged.

Forbidden at tree-level

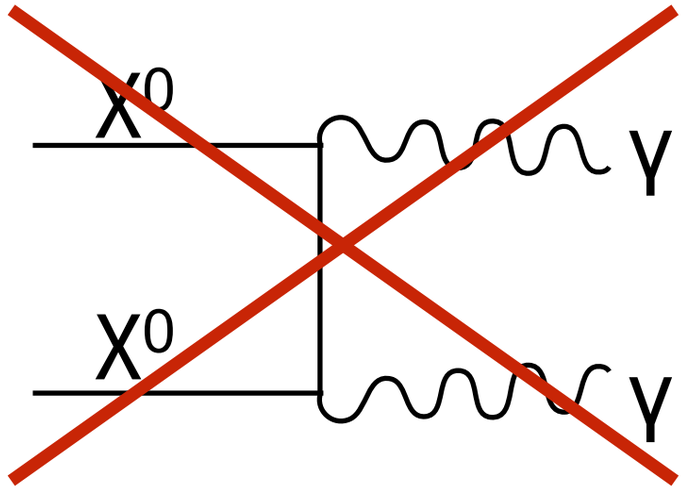

One-loop

$$\sim \sqrt{2}\frac{\alpha_W m_\chi}{m_W}$$

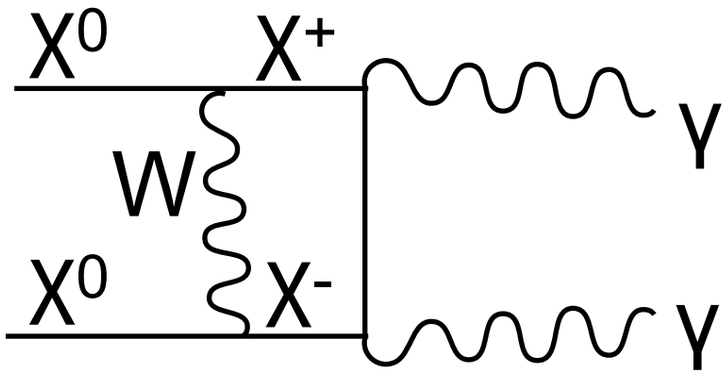

Long-range potential

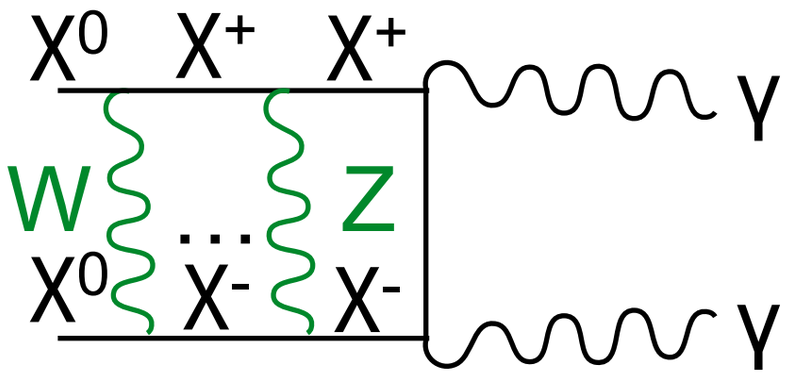

The wino potential

evolution equation for two-particle state

$$i\partial_t \Psi = H^0 \Psi = \left[-\frac{\nabla_X^2}{4M_\chi} - \frac{\nabla_r^2}{M_\chi} + V(r) \right] \Psi$$

evolution preserves total charge; need only consider Q=0 two-body states

$$\Psi = \begin{pmatrix} \psi_N \, (\equiv \chi^0 \chi^0) \\ \psi_C \, (\equiv \chi^+ \chi^-) \end{pmatrix}$$

potential V(r) for initial-state winos couples $\chi^0\chi^0$ and $\chi^+\chi^-$ states through *W* exchange; $\chi^+\chi^-$ state experiences Z and photon exchange

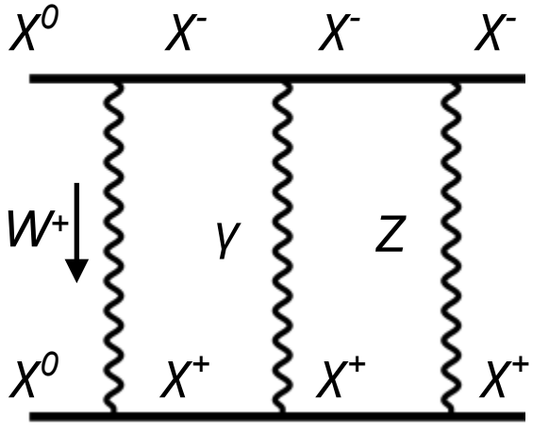

$$V(r) = \begin{pmatrix} 0 & -\sqrt{2}\alpha_W \frac{e^{-m_W r}}{r} \\ -\sqrt{2}\alpha_W \frac{e^{-m_W r}}{r} & 2\delta M - \frac{\alpha}{r} - \alpha_W c_W^2 \frac{e^{-m_Z r}}{r} \end{pmatrix}$$

Potential-enhanced annihilation

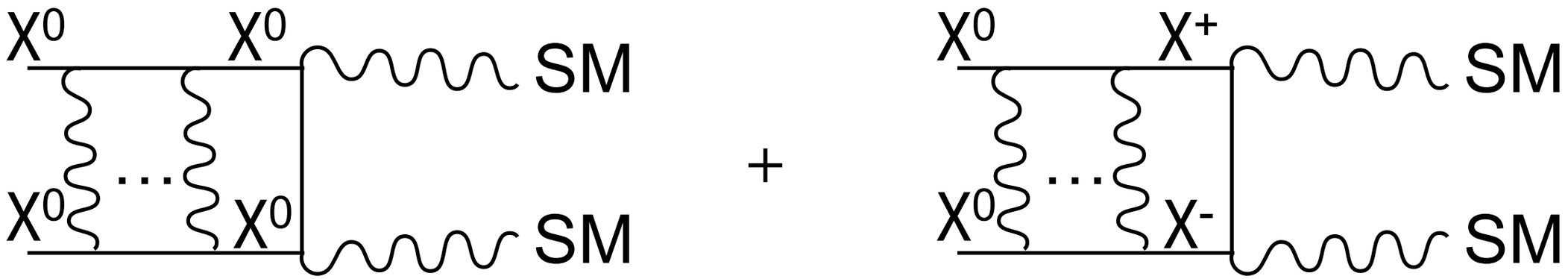

- For general final states, two interfering sets of ladder diagrams, distinguished by annihilating state at “last rung” of ladder: $\chi^0\chi^0$ vs $\chi^+\chi^-$ [e.g. Hisano et al ’04].
- Overall amplitude is the sum of these terms, each one built from the hard matrix element + a Sommerfeld factor:

$$A_{\chi^0\chi^0\to X} = s_{00} A^0_{\chi^0\chi^0\to X} + s_{0\pm} A^0_{\chi^+\chi^-\to X}$$

- Sommerfeld “s” factors describe wavefunction distortion. At low DM mass, where potential is perturbative, $s_{00} >> s_{0\pm}$ (~1 vs $O(\alpha_W)$). But at high DM mass, they are of the same order - lifts suppression for annihilation to photons.

Potential-enhanced annihilation

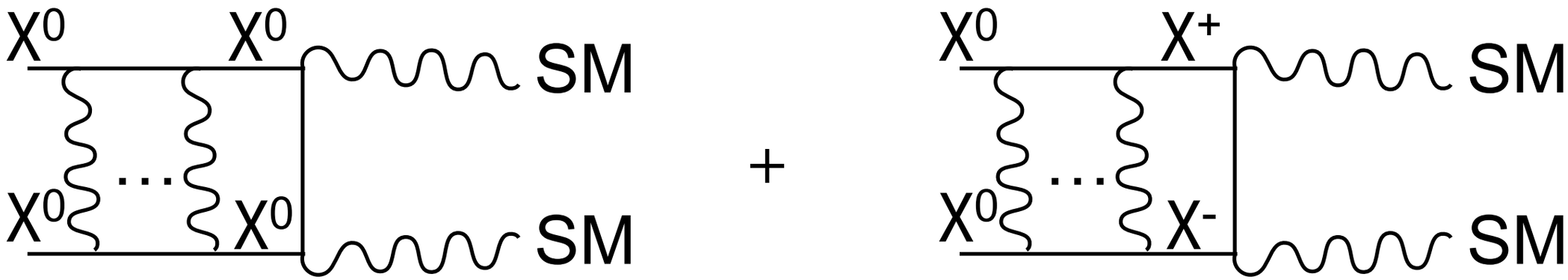

- For general final states, two interfering sets of ladder diagrams, distinguished by annihilating state at "last rung" of ladder: $\chi^0\chi^0$ vs $\chi^+\chi^-$ [e.g. Hisano et al '04].

- Overall amplitude is the sum of these terms, each one built from the hard matrix element + a Sommerfeld factor:

$$A_{\chi^0\chi^0\to X} = s_{00}A^0_{\chi^0\chi^0\to X} + s_{0\pm}A^0_{\chi^+\chi^-\to X}$$

Sommerfeld factors determined from wavefunction at origin

$$s_{00} = \psi_N(0), s_{0\pm} = \psi_C(0)$$

- Sommerfeld "s" factors describe wavefunction distortion. At low DM mass, where potential is perturbative, $s_{00} >> s_{0\pm}$ (~1 vs $O(\alpha_W)$). But at high DM mass, they are of the same order - lifts suppression for annihilation to photons.

Potential-enhanced annihilation

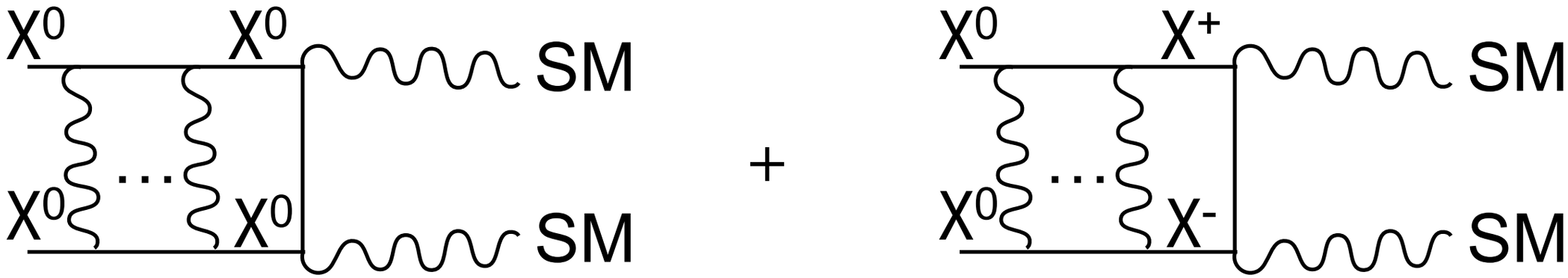

- For general final states, two interfering sets of ladder diagrams, distinguished by annihilating state at "last rung" of ladder: $\chi^0\chi^0$ vs $\chi^+\chi^-$ [e.g. Hisano et al '04].

- Overall amplitude is the sum of these terms, each one built from the hard matrix element + a Sommerfeld factor:

$$A_{\chi^0\chi^0\to X} = s_{00}A^0_{\chi^0\chi^0\to X} + s_{0\pm}A^0_{\chi^+\chi^-\to X}$$

fixed-order calculations not reliable for thermal wino - calculate using SCET

- Sommerfeld "s" factors describe wavefunction distortion. At low DM mass, where potential is perturbative, $s_{00} >> s_{0\pm}$ (~1 vs $O(\alpha_W)$). But at high DM mass, they are of the same order - lifts suppression for annihilation to photons.

Two subtleties

- Not sufficient to only compute the gamma-ray line amplitude (DM DM → γγ), need the full gamma-ray spectrum around the endpoint (DM DM → γ + X)

  - Instruments have finite energy resolution (~10% for best current telescope) - cannot cleanly separate line

- Best constraints come from likelihood analysis, require signal model + background model

- For correct limit, cannot treat energy resolution as a sharp cutoff - need to obtain full differential spectrum, convolve with energy resolution function, compare to observed data

Two subtleties

- Limits are really on photon flux - cross section is degenerate with amount of DM near GC, which has large uncertainties
  - N-body simulations suggest DM density should rise toward GC (roughly as 1/r), but flatten out at some “core” radius
  - Core size depends on details of baryonic physics - but from current simulations, expected to be ~1-2 kpc or smaller in the Milky Way
  - Distance from Earth to GC is ~8.5 kpc

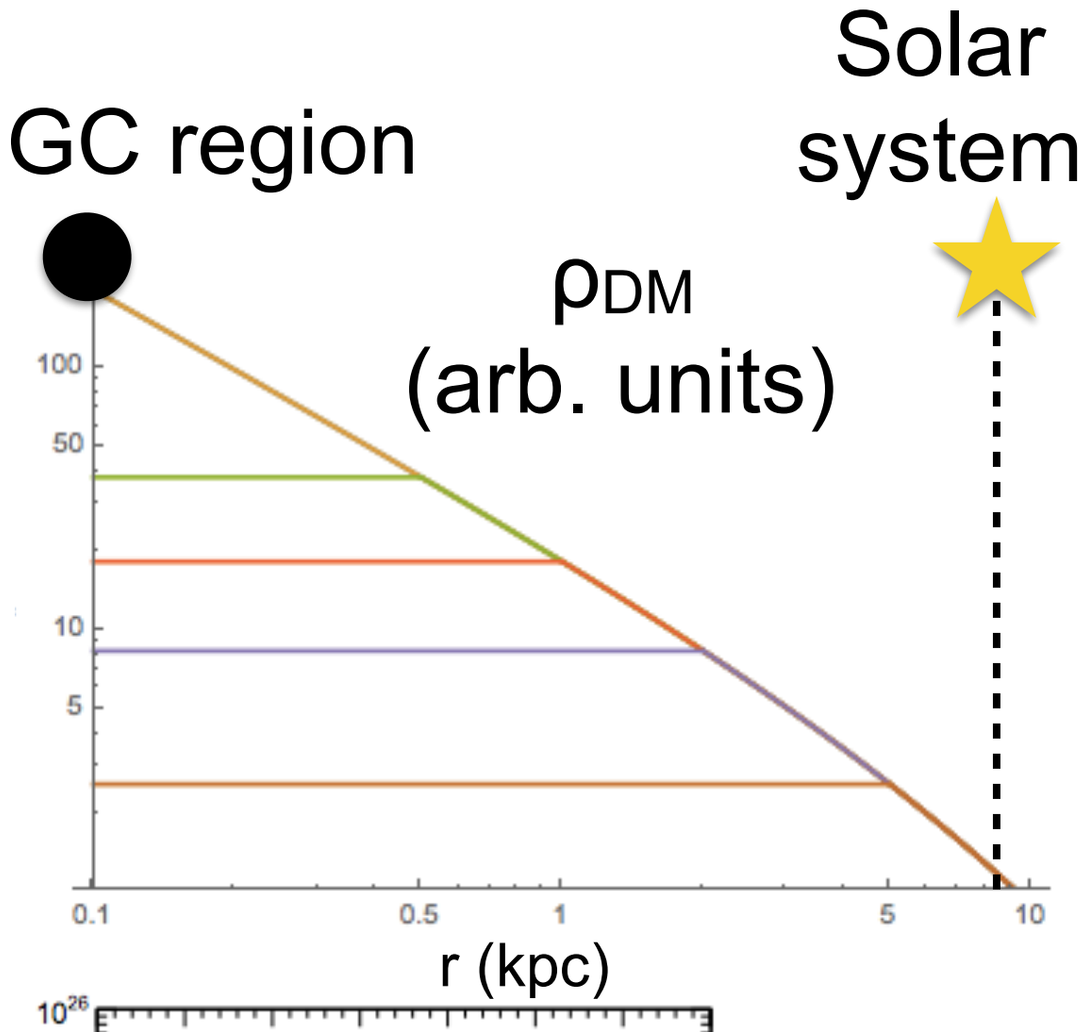

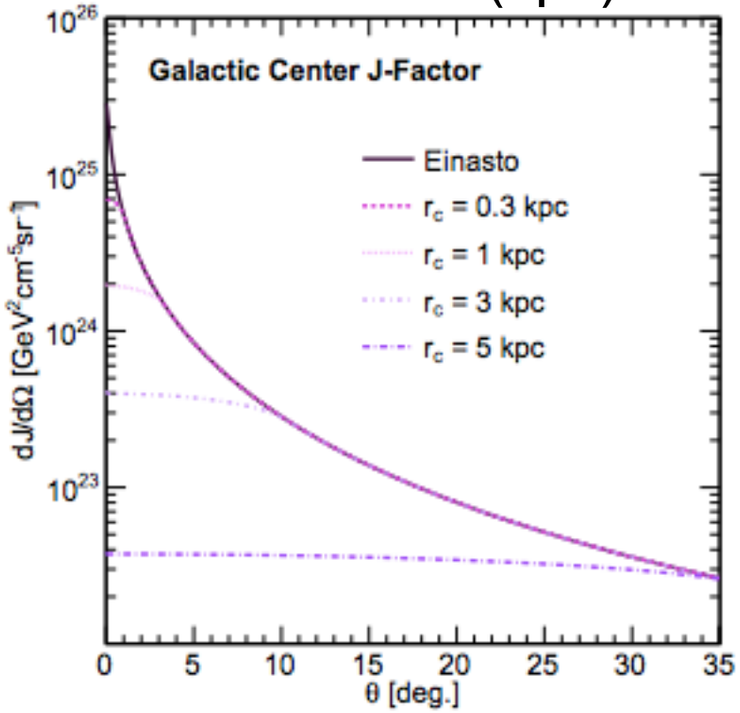

Two subtleties

- Limits are really on photon flux - cross section is degenerate with amount of DM near GC, which has large uncertainties
  - N-body simulations suggest DM density should rise toward GC (roughly as 1/r), but flatten out at some “core” radius
  - Core size depends on details of baryonic physics - but from current simulations, expected to be ~1-2 kpc or smaller in the Milky Way
  - Distance from Earth to GC is ~8.5 kpc

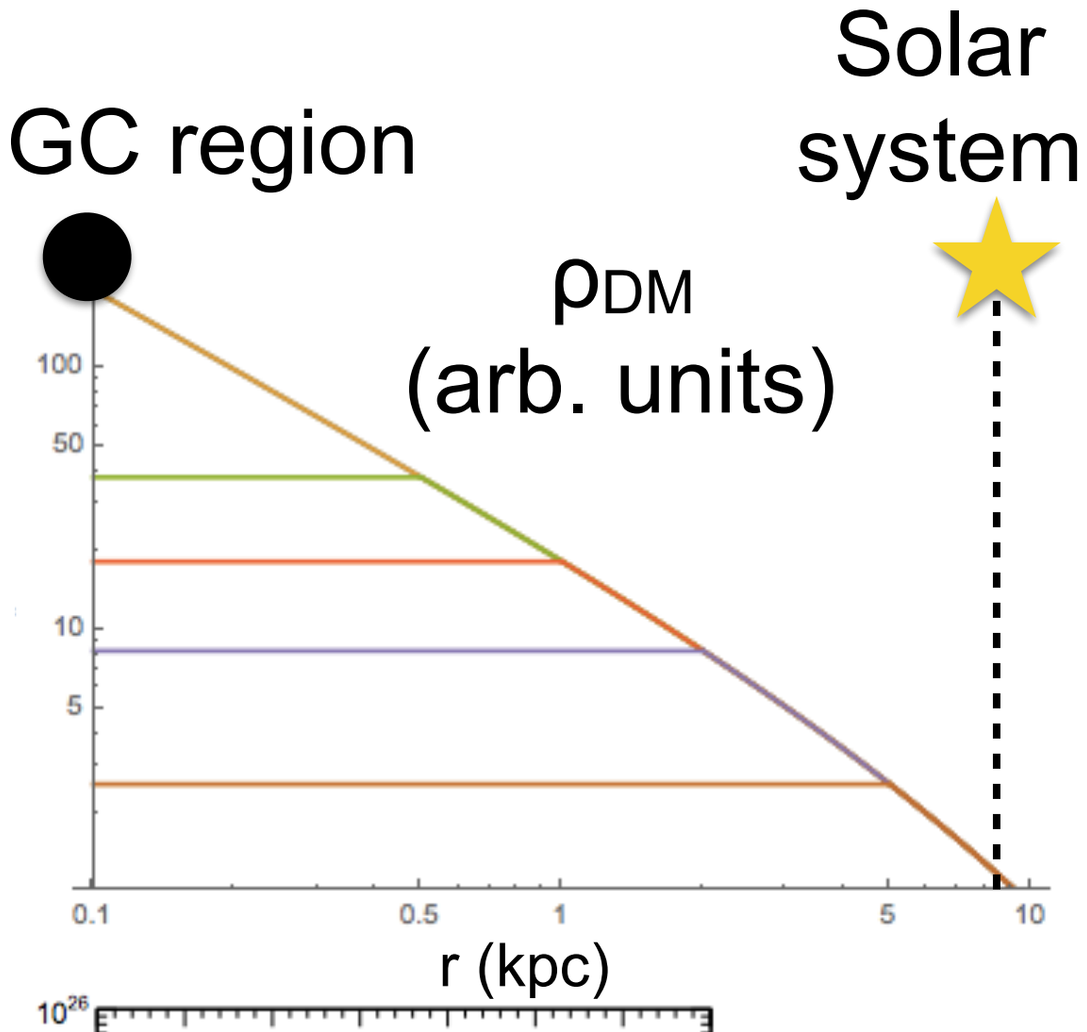

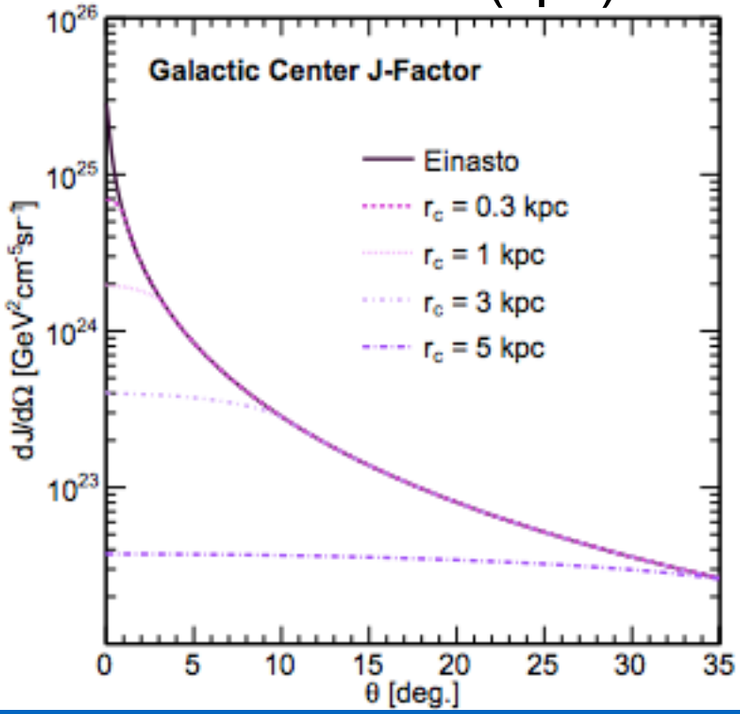

can we constrain the “thermal wino + 1-2 kpc core” scenario?

Three regions

$$z \equiv E_\gamma / m_\chi \qquad m_X^2 = 4m_\chi^2(1-z)$$

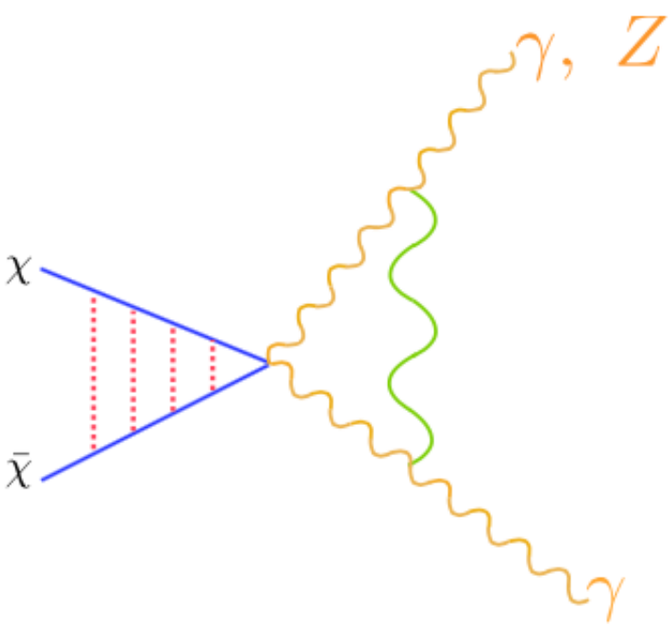

(a)

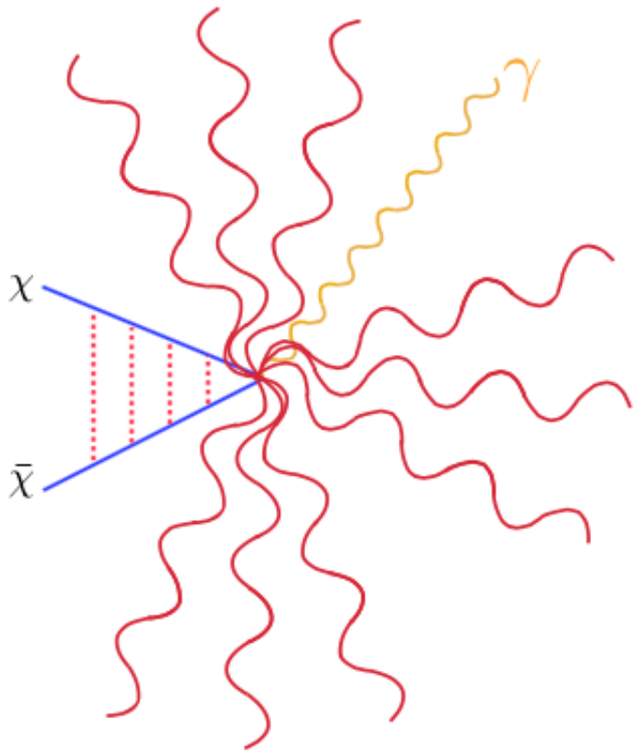

(b)

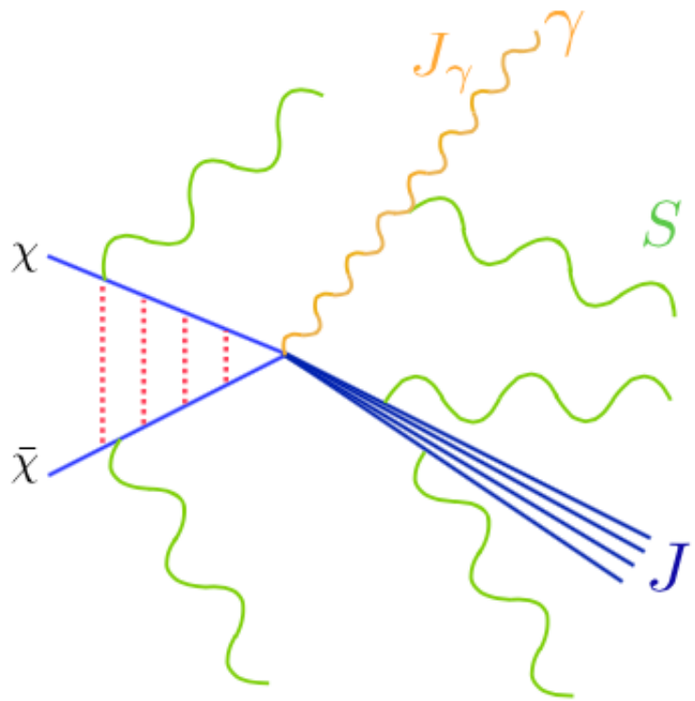

(c)

Exclusive

2→2 annihilation

γγ, γZ final states

Cohen et al ’15; Ovanesyan, TRS & Stewart ’15; Ovanesyan, Rodd, TRS & Stewart ‘17

Semi-inclusive

Integrate out recoil state X

γ+X final state, X heavy

Baumgart et al ‘15a,b; Baumgart & Vaidya ‘16

Endpoint region

Recoil state forced into jet

γ+X final state

Baumgart, TRS et al, ’18,’19

For the regime even closer to the endpoint, see Beneke et al ’18,’19

Three regions

we recover these previous cases as limits

$$z \equiv E_\gamma / m_\chi \qquad m_X^2 = 4m_\chi^2(1-z)$$

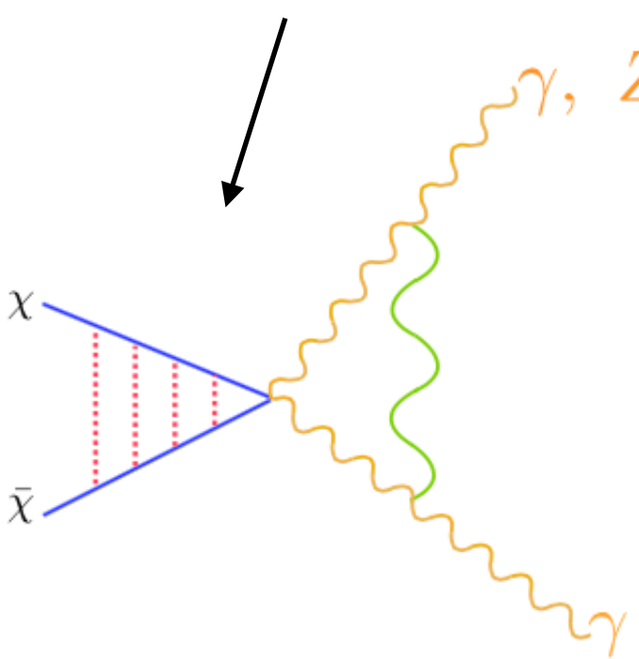

(a)

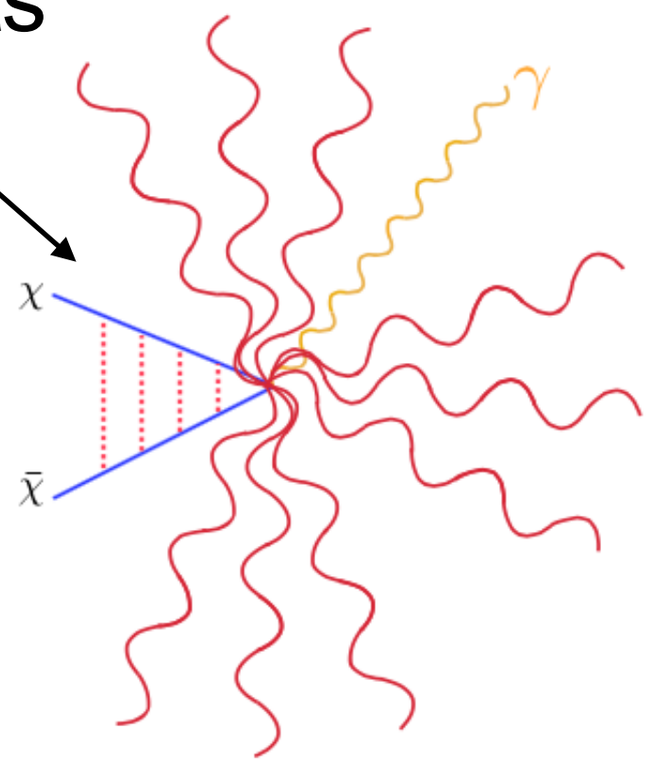

(b)

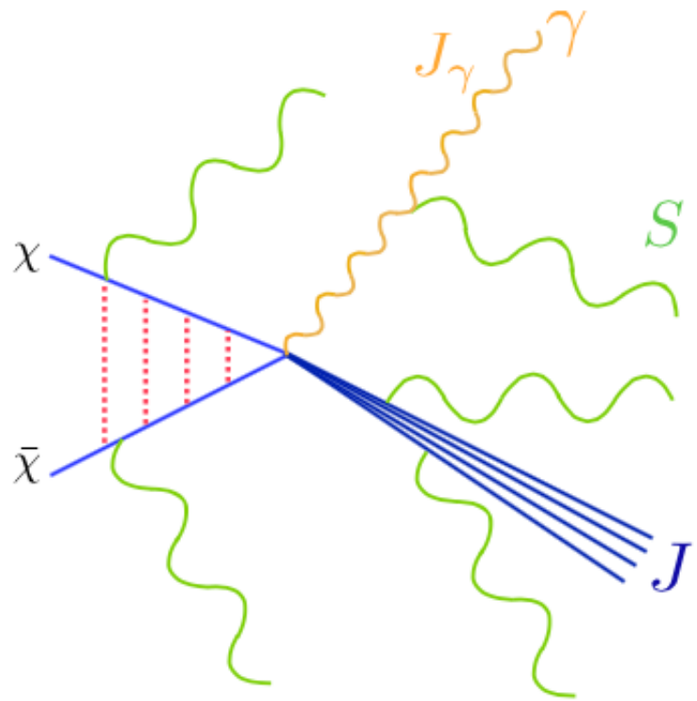

(c)

Exclusive

2→2 annihilation

γγ, γZ final states

Cohen et al ’15; Ovanesyan, TRS & Stewart ’15; Ovanesyan, Rodd, TRS & Stewart ‘17

Semi-inclusive

Integrate out recoil state X

γ+X final state, X heavy

Baumgart et al ‘15a,b; Baumgart & Vaidya ‘16

Endpoint region

Recoil state forced into jet

γ+X final state

Baumgart, TRS et al, ’18,’19

For the regime even closer to the endpoint, see Beneke et al ’18,’19

Mode structure in the endpoint regime

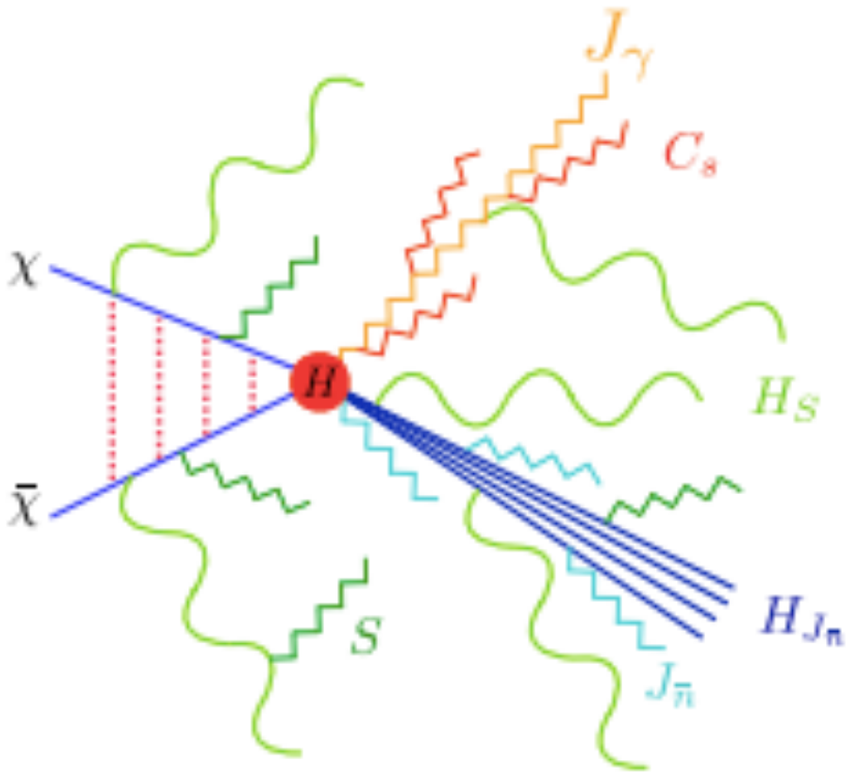

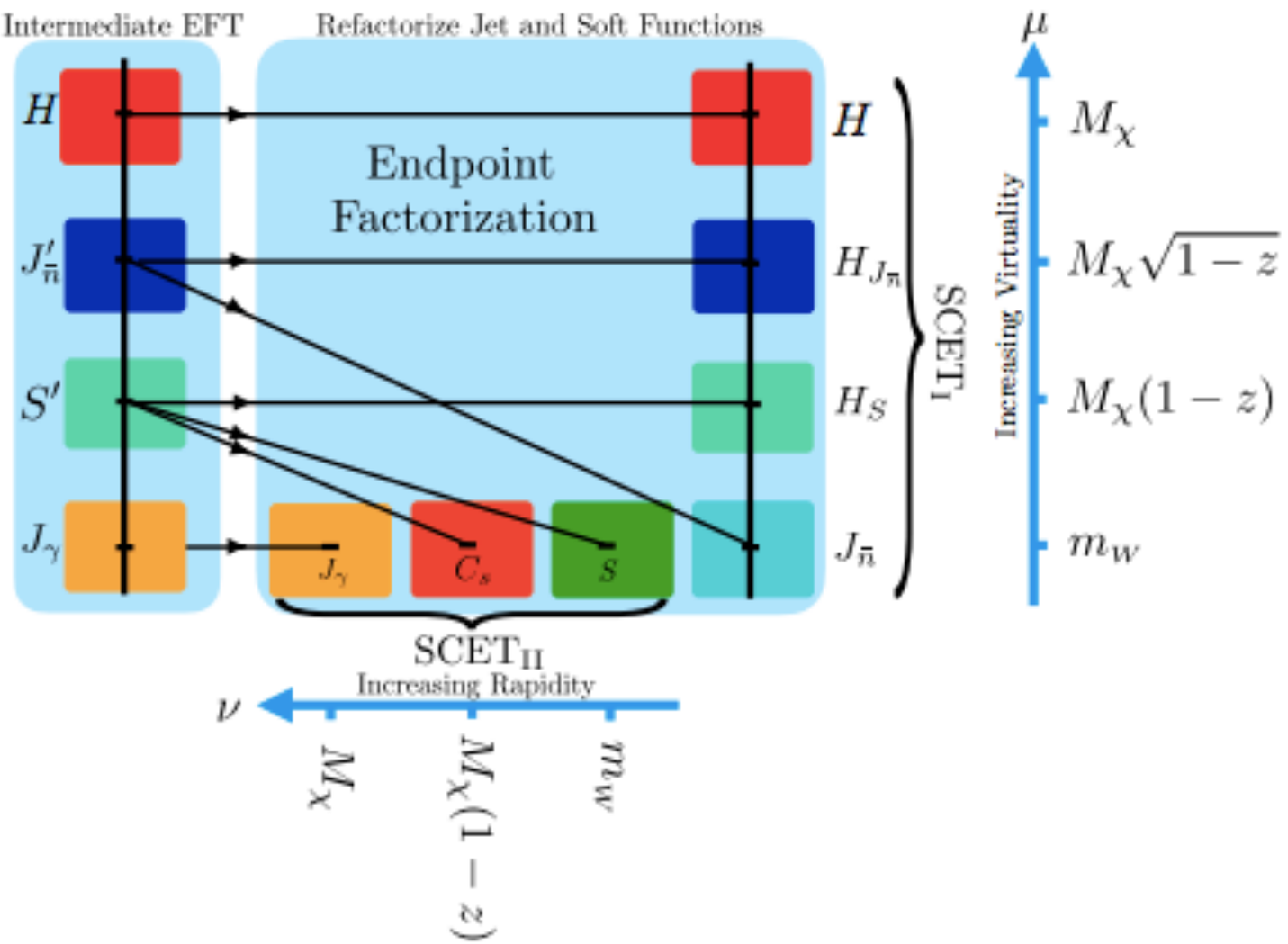

curvy lines = unbroken theory
zigzag = sensitive to m_W

- Two relevant small scales - EW symmetry breaking (m_W) and separation from endpoint (controlled by z)
- Need two-stage factorization, modes separated by both virtuality and rapidity

Stage 1: factorization in SCET$_{\rm I}$

- Small parameter: $\lambda = \sqrt{1-z}$

- Using SCET$_{\rm I}$ formalism, cross section factorizes into hard, ultrasoft, collinear-jet contributions. Modes are:

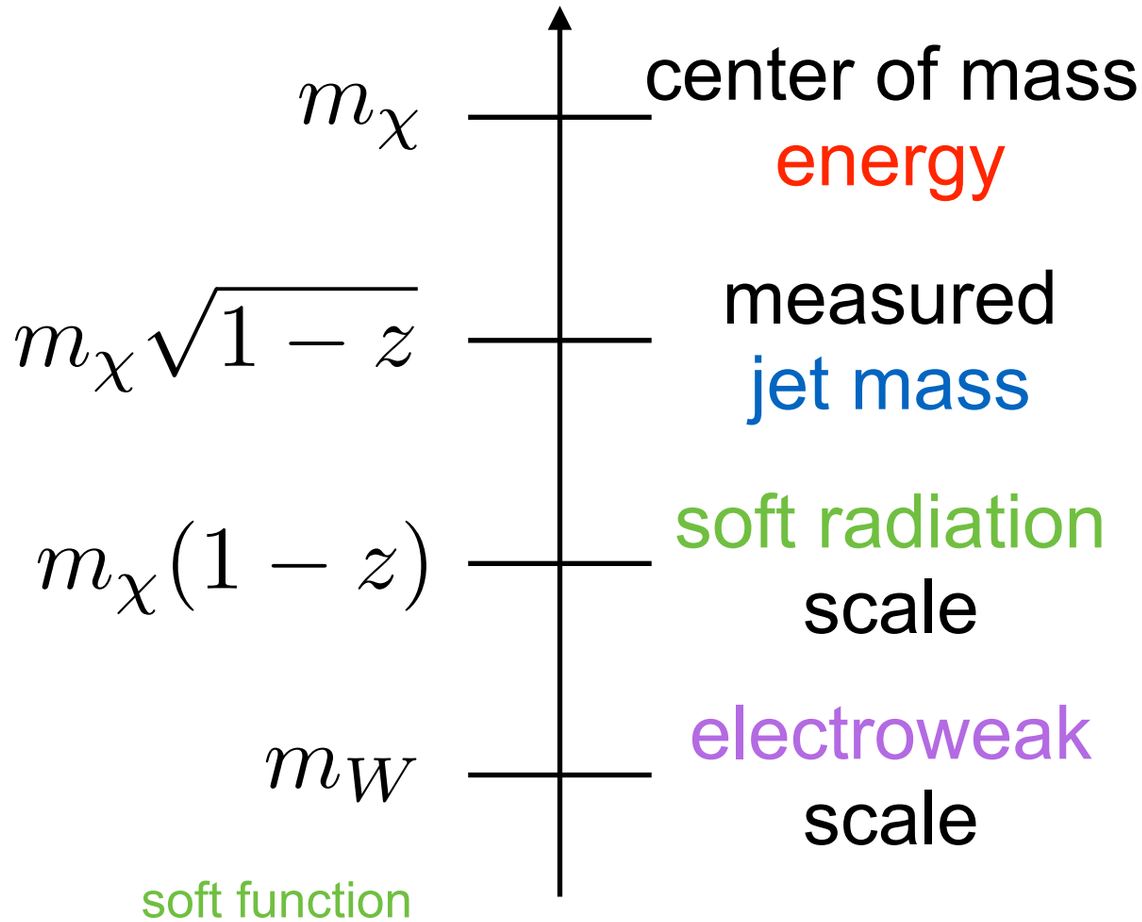

$$p_c \sim M_\chi(1, \lambda^2, \lambda), \qquad p_{us} \sim M_\chi(\lambda^2, \lambda^2, \lambda^2)$$

hard function; photon jet function; recoiling jet function; soft function

$$\frac{\mathrm{d}\hat{\sigma}}{\mathrm{d}z} = H_{ij}(M_\chi)\, J_\gamma(m_W)\, J'_{\bar{n}}(M_\chi, 1-z, m_W) \otimes S'_{ij}(1-z, m_W)$$

- Still need to disentangle scale dependences in soft function and jet function, break into modes with simple virtuality/rapidity scaling. Use SCET$_{\rm II}$ for this.

Stage 2: refactorization

- For the jet function, two types of collinear modes, corresponding to the two low scales; allows factorization of jet function into (piece depending on z) x (piece depending on m_W).

$$J'_{\bar{n}}\left(M_\chi, \sqrt{1-z}, m_W, \mu\right) = H_{J_{\bar{n}}}\left(M_\chi, \sqrt{1-z}, \mu\right) J_{\bar{n}}\left(m_W, \mu, \nu\right) + \mathcal{O}\left(\frac{m_W}{M_\chi\sqrt{1-z}}\right)$$

- Soft function is more complicated - collinear-soft modes are required to capture all divergences:

$$p_{c_S} \sim M_\chi(1-z)(\lambda^2, 1, \lambda)\,, \qquad \lambda = \frac{m_W}{M_\chi(1-z)}\,.$$

- Hilbert space factorizes into soft (with $\lambda = m_W/m_\chi$) and collinear-soft modes (the latter scaling with both m_W and z).

$$S'^{\,aba'b'}_i\left(M_\chi, 1-z, m_W\right) = H_{S,ij}\left(M_\chi, 1-z, \mu\right)\left[C_S\left(M_\chi, 1-z, m_W, \mu, \nu\right) S\left(m_W, \mu\right)\right]^{aba'b'}_j$$

Structure of the resummed result

zigzag = modes sensitive to electroweak symmetry breaking

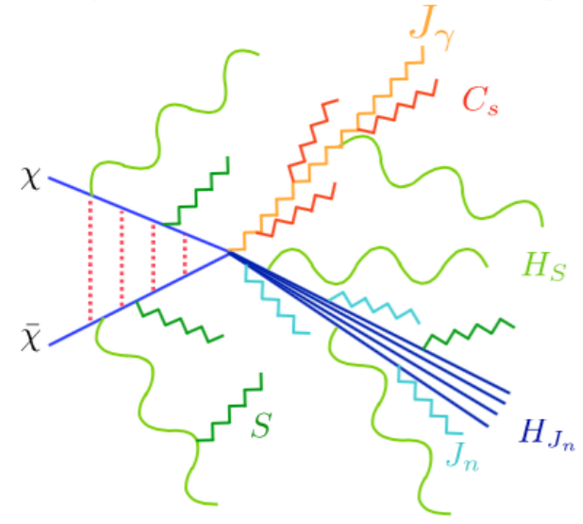

$$\left(\frac{\mathrm{d}\hat{\sigma}}{\mathrm{d}z}\right)^{\mathrm{NLL}} = H(M_\chi,\mu)\, J_\gamma(m_W,\mu,\nu)\, J_{\bar{n}}(m_W,\mu,\nu)\, S(m_W,\mu,\nu)$$

$$\times H_{J_{\bar{n}}}(M_\chi,1-z,\mu) \otimes H_S(M_\chi,1-z,\mu) \otimes C_S(M_\chi,1-z,m_W,\mu,\nu)\,.$$

- We proved a factorization theorem that is valid to NLL, allowing the cross section to be separated into functions describing physics at different scales.

- $H(M_\chi,\mu)$: this hard function captures virtual corrections for $\chi\chi \to \gamma\gamma, \gamma Z$.
- $H_{J_{\bar{n}}}(M_\chi,1-z,\mu)$: this jet function captures the collinear radiation at the scale $M_\chi\sqrt{1-z}$.
- $H_S(M_\chi,1-z,\mu)$: this soft function captures soft radiation at the scale $M_\chi(1-z)$.

do not depend on EWSB, can be evaluated in unbroken theory

- $J_\gamma(m_W,\mu,\nu)$: this photon jet function captures the virtual corrections to the outgoing γ.
- $S(m_W,\mu,\nu)$: this soft function captures wide angle soft radiation at the electroweak scale.
- $J_{\bar{n}}(m_W,\mu,\nu)$: this jet function captures collinear radiation in X at the electroweak scale.
- $C_S(M_\chi,1-z,m_W,\mu,\nu)$: this collinear-soft function captures radiation along the γ direction.

sensitive to low scale m_W, must be evaluated in broken theory.

RG evolution path

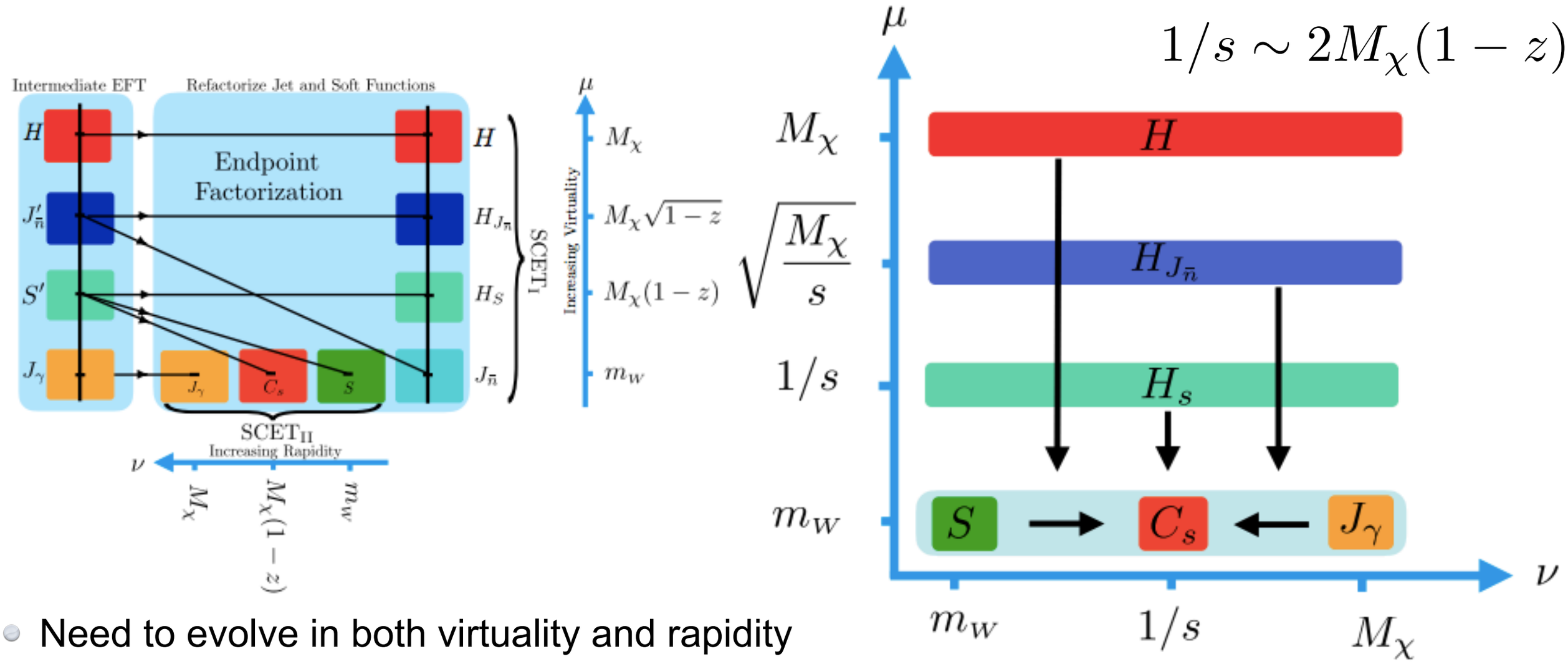

- Need to evolve in both virtuality and rapidity
- At μ=m_W, we find the relevant parts (for NLL) of the rapidity anomalous dimensions vanish - trivial to evolve in rapidity at μ=m_W
- Simplest path thus runs H/H_{Jn}/H_s functions down to μ~m_W, then rapidity evolution to v~1/s is trivial

The LL final spectrum

Baumgart, Cohen, Moult, Rodd, Solon, TRS, Stewart & Vaidya ‘18

$$\frac{\mathrm{d}\sigma^{\mathrm{LL}}}{\mathrm{d}z} = 4\,|s_{0\pm}|^2\,\sigma^{\mathrm{tree}}\,e^{-2\,\Gamma_0\,\tilde{\alpha}_W\,L_\chi^2}\,\delta(1-z)$$

$$+\,4\,\sigma^{\mathrm{tree}}\,e^{-2\,\Gamma_0\,\tilde{\alpha}_W\,L_\chi^2}\Big\{C_A\,\tilde{\alpha}_W\,F_1\Big(3\,\mathcal{L}_1^S(z)-2\,\mathcal{L}_1^J(z)\Big)\,e^{2\,\Gamma_0\,\tilde{\alpha}_W\,\left(\Theta_J L_J^2(z)-\frac{3}{4}\Theta_S L_S^2(z)\right)}$$

$$-\,2\,C_A\,\tilde{\alpha}_W\,F_0\,\mathcal{L}_1^J(z)\,e^{2\,\Gamma_0\,\tilde{\alpha}_W\,L_J^2(z)}\Big\}. \qquad (5.30)$$

$$\Gamma_0 = 4\,C_A \qquad \tilde{\alpha}_W = \frac{\alpha_W}{4\pi}$$

$$L_J(z) = \log\left(\frac{m_W}{2\,M_\chi\sqrt{1-z}}\right) \quad L_S(z) = \log\left(\frac{m_W}{2\,M_\chi(1-z)}\right) \quad L_\chi = \log\left(\frac{m_W}{2\,M_\chi}\right)$$

$$\Theta_J = \Theta\left(1-\frac{m_W^2}{4\,M_\chi^2}-z\right)$$

$$\Theta_S = \Theta\left(1-\frac{m_W}{2\,M_\chi}-z\right)$$

large logs

$$\sigma^{\mathrm{tree}} = \frac{\pi\,\alpha_W^2\,\sin^2\theta_W}{2\,M_\chi^2\,v}$$

tree-level cross section

$$\mathcal{L}_1^J(z) = \frac{L_J}{1-z}\,\Theta_J\,, \quad \mathcal{L}_1^S(z) = \frac{L_S}{1-z}\,\Theta_S$$

power divergences in (1-z)

$$F_0 = \frac{4}{3}\,|s_{00}|^2 + 2\,|s_{0\pm}|^2 + \frac{2\sqrt{2}}{3}\left(s_{00}\,s_{0\pm}^* + s_{00}^*\,s_{0\pm}\right),$$

$$F_1 = -\frac{4}{3}\,|s_{00}|^2 + 2\,|s_{0\pm}|^2 - \frac{2\sqrt{2}}{3}\left(s_{00}\,s_{0\pm}^* + s_{00}^*\,s_{0\pm}\right),$$

Sommerfeld factors

At NLL, the power-law terms are dressed with additional logs.

Results for the resummed spectrum

Baumgart, Cohen, Moulin, Moult, Rinchiuso, Rodd, TRS, Stewart & Vaidya ‘19

- We have computed the full resummed spectrum analytically to next-to-leading-log (NLL) [Baumgart, TRS et al ‘19], including the Sommerfeld enhancement; we previously computed the spectrum to LL [Baumgart, TRS et al ’18].

- Our theory uncertainties are now at the level of 5%.

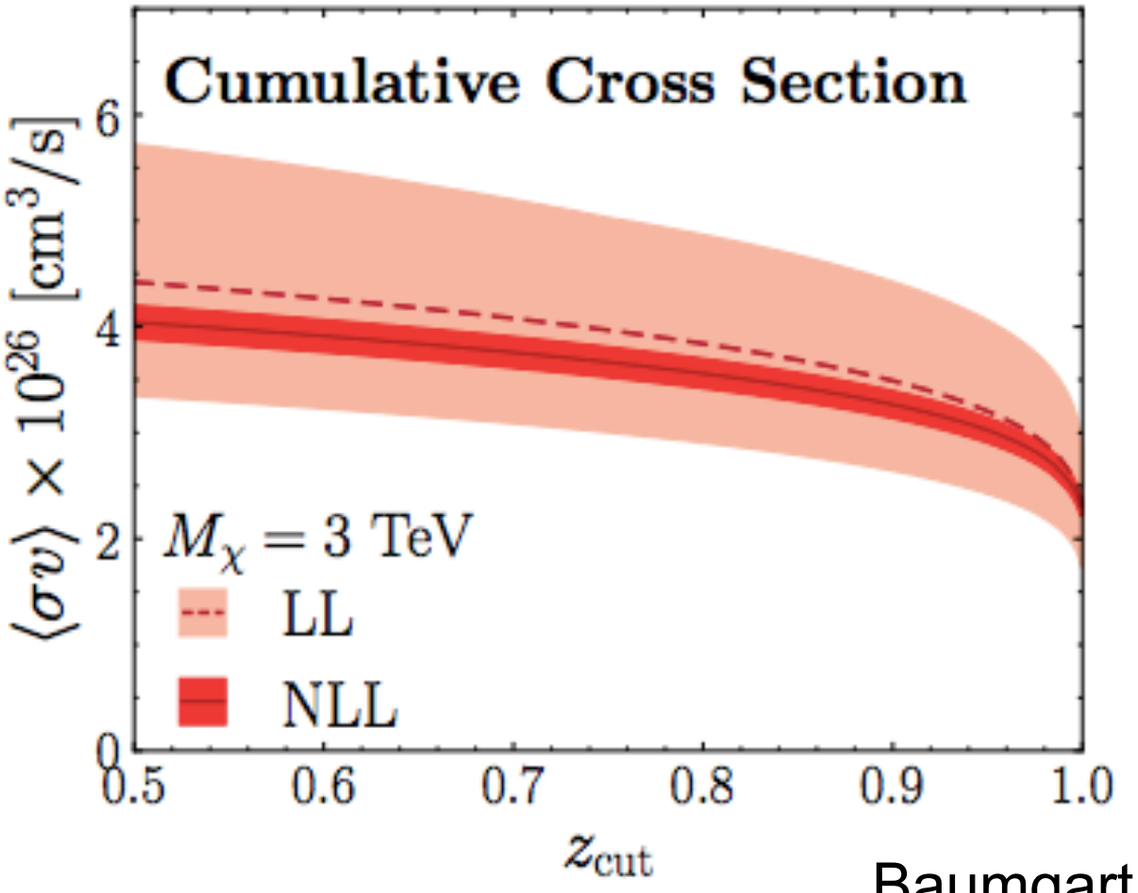

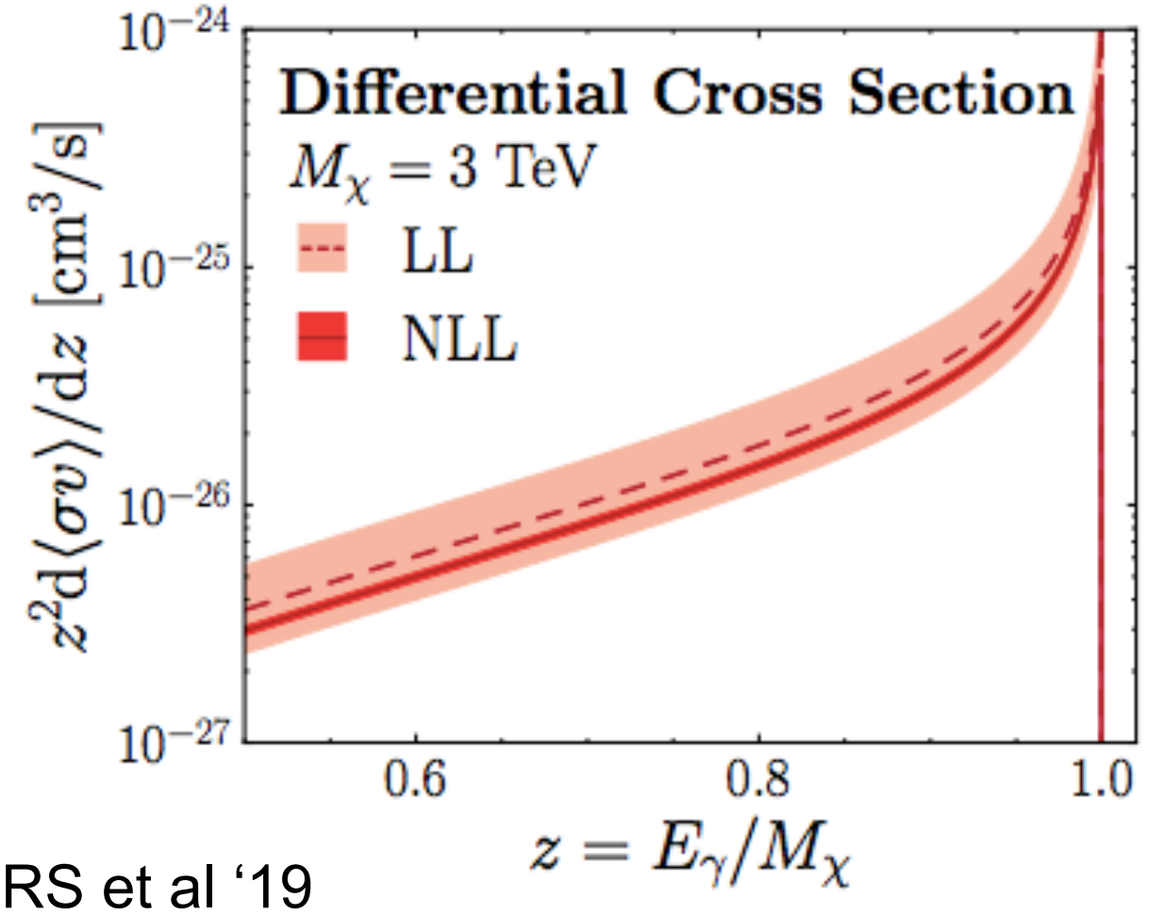

Baumgart, TRS et al ‘19

Hunting the wino with H.E.S.S

Rinchiuso, Rodd, Moult, Moulin, Baumgart, Cohen, TRS, Stewart & Vaidya ‘18

- In work led by Lucia Rinchiuso (H.E.S.S), we have forecast the constraints that current and future H.E.S.S Galactic Center data could set on thermal winos.
- We consider a range of choices for the core radius, simulate backgrounds from cosmic rays and known gamma-ray sources, and account for the H.E.S.S. energy resolution.
- We perform a likelihood analysis on simulated data, binned in energy + distance from the Galactic Center.

Spatial regions tested

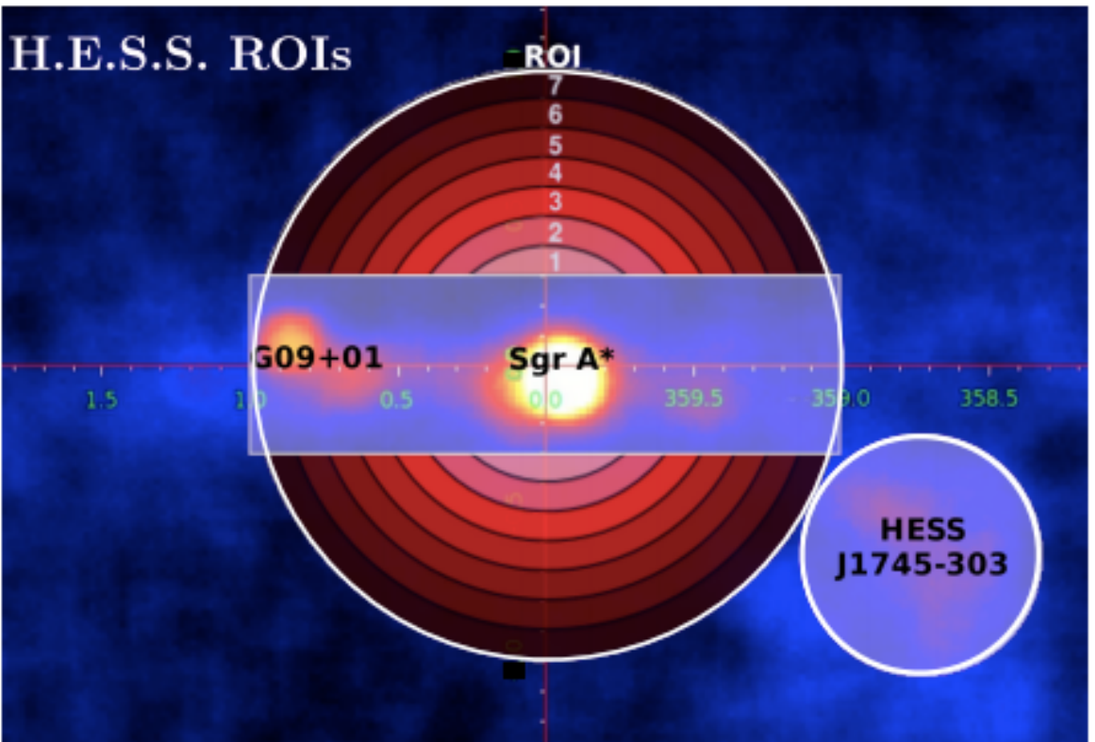

Example signal & background

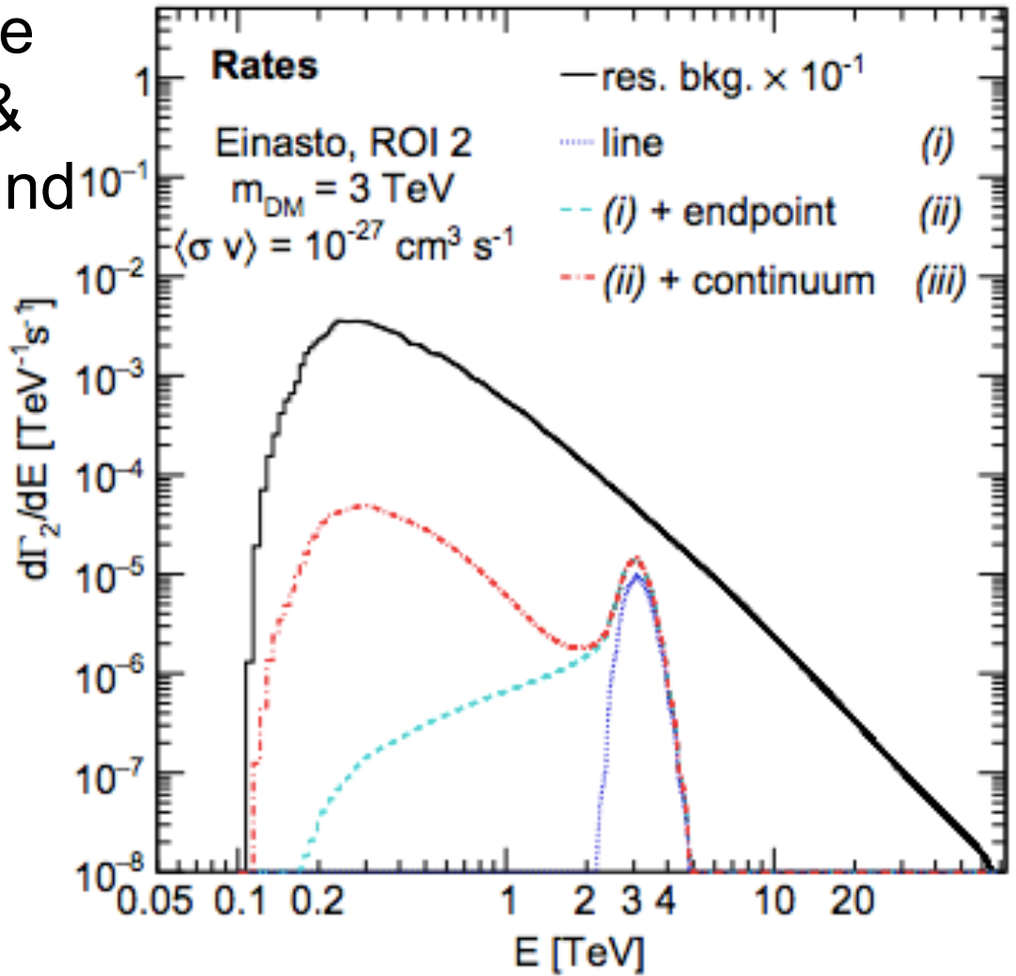

Forecast limits

can we constrain the “thermal wino + 1-2 kpc core” scenario?

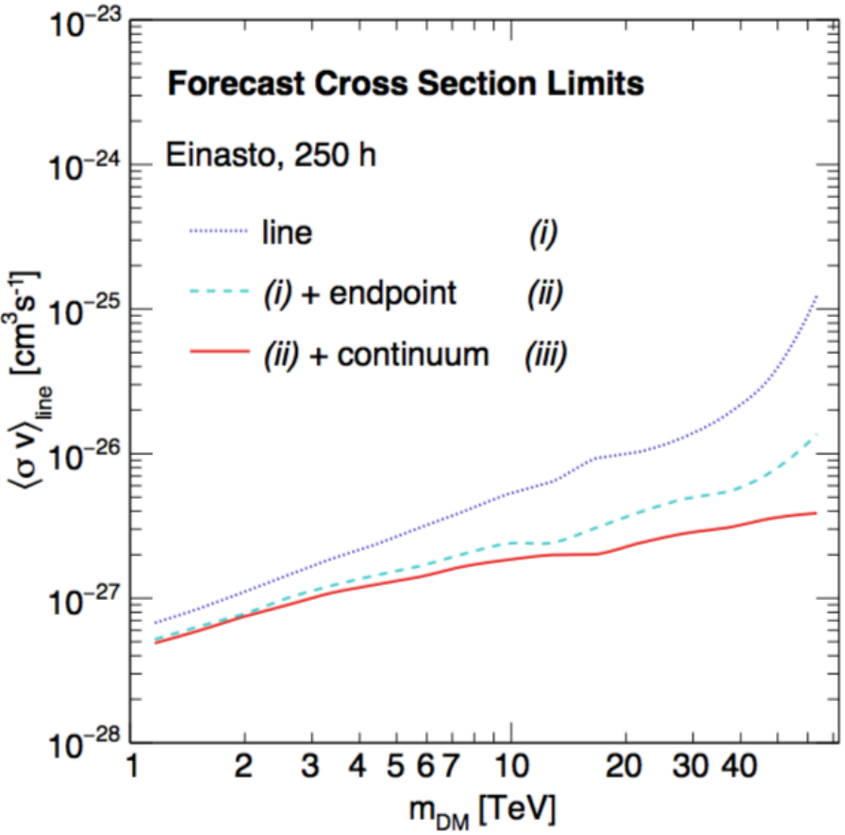

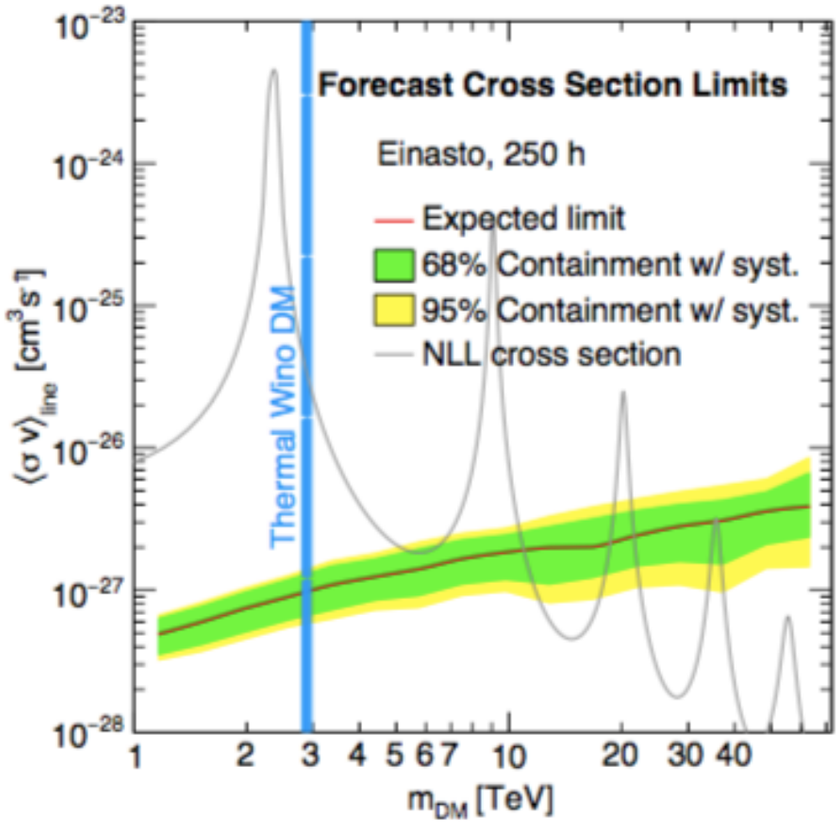

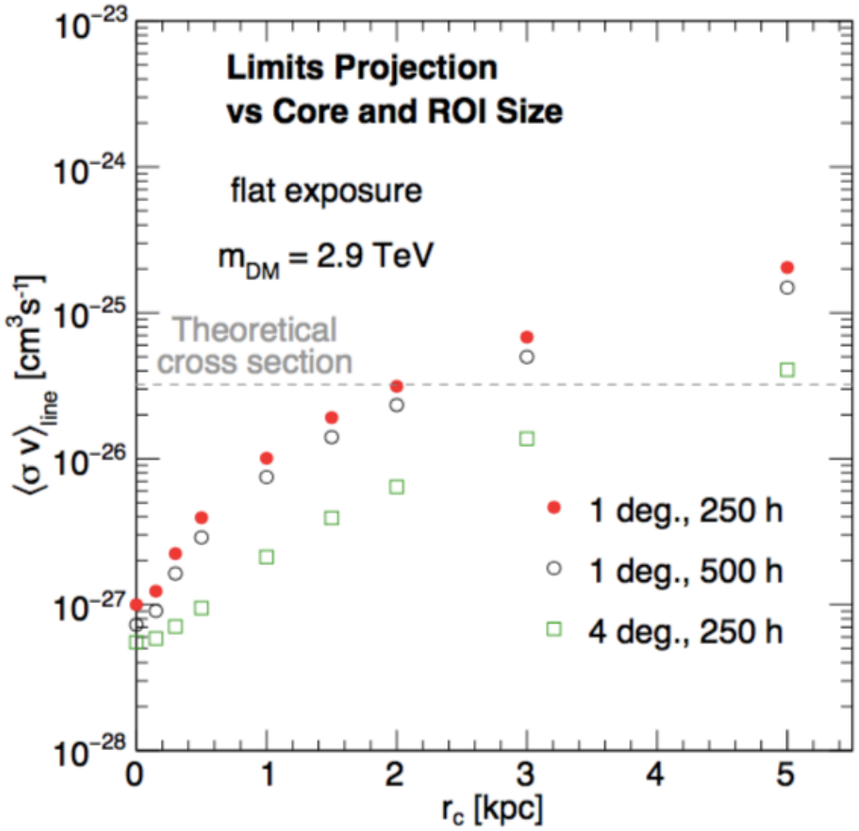

- Using full spectrum (vs resummed line) improves limits by a factor ~1.5 for thermal wino.
- Analysis of current data could exclude thermal wino DM with core radius below 2 kpc.
- New “Inner Galaxy Survey” strategy by H.E.S.S could test nearly 5kpc core sizes.

Forecast limits

can we constrain the “thermal wino + 1-2 kpc core” scenario?

yes!

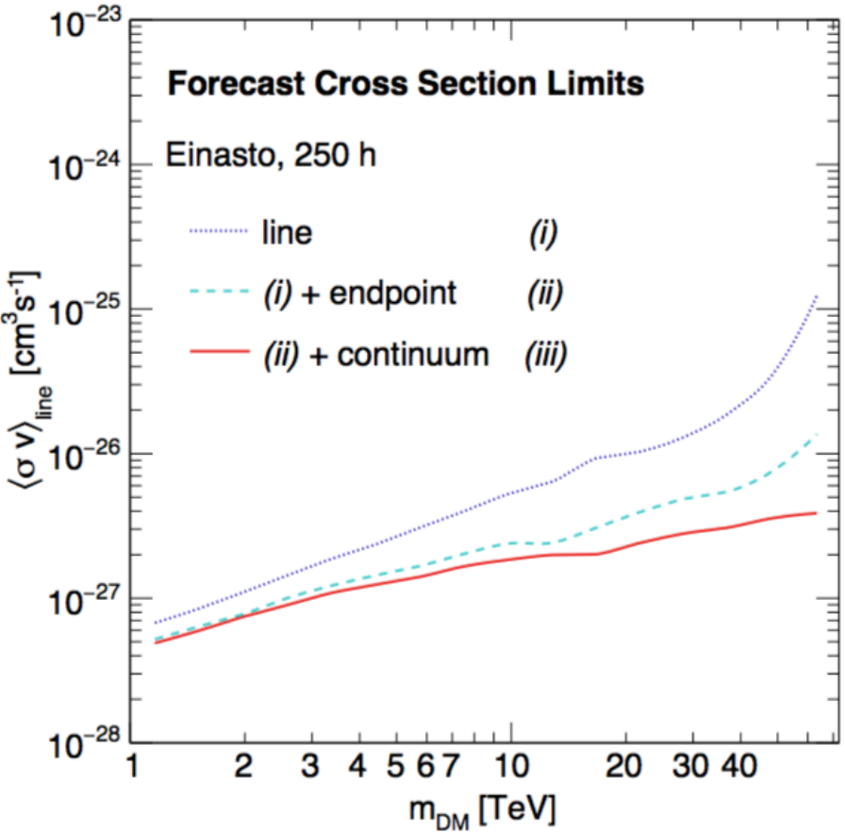

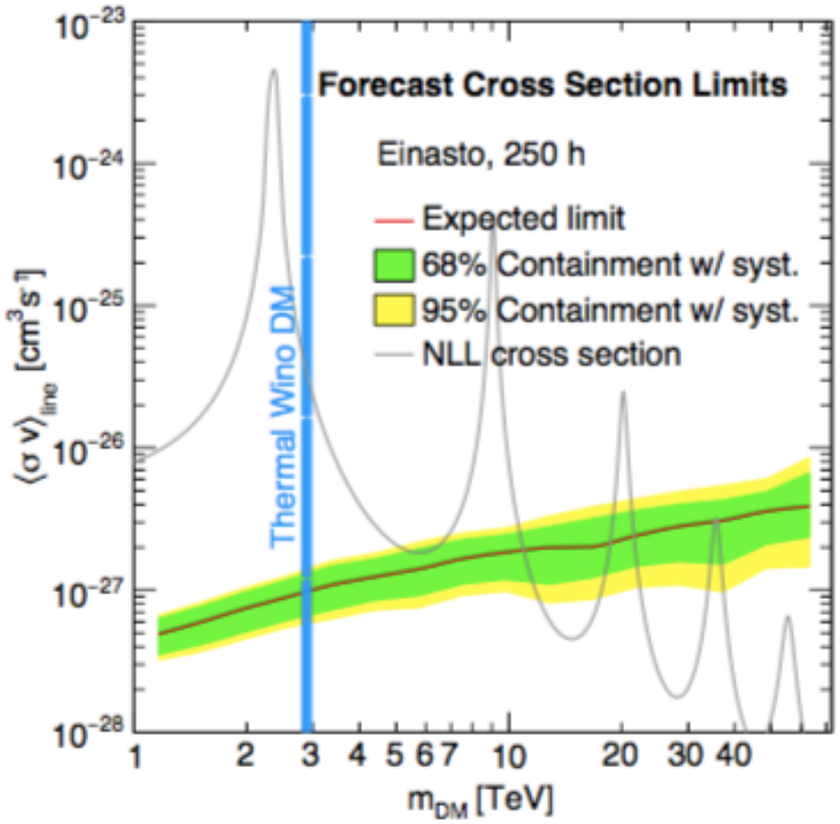

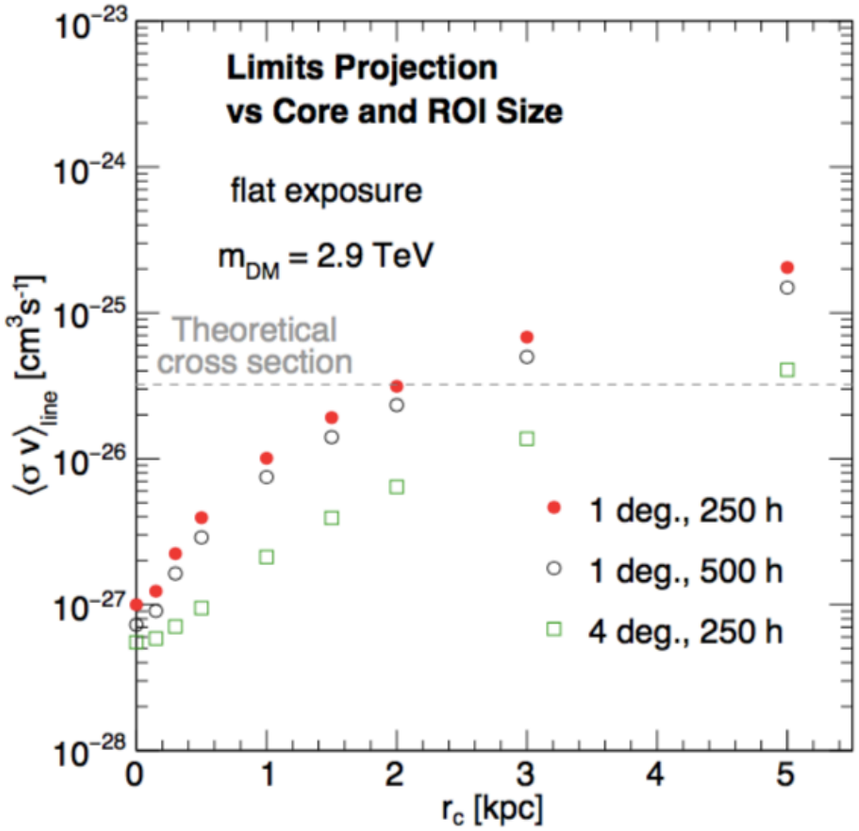

- Using full spectrum (vs resummed line) improves limits by a factor ~1.5 for thermal wino.
- Analysis of current data could exclude thermal wino DM with core radius below 2 kpc.
- New “Inner Galaxy Survey” strategy by H.E.S.S could test nearly 5kpc core sizes.

Summary

- SU(2) triplet (wino) DM is very simple and predictive, and not yet excluded by colliders or direct detection. Also shares similar interesting non-perturbative physics with dark sectors with light dark forces.

- We have calculated the first resummed hard photon spectrum from heavy wino annihilation, now to NLL (5% theoretical uncertainties, comparable to experimental systematics) - incorporates and supersedes earlier calculations.

- SCET techniques should be broadly applicable to models of heavy DM coupled to lighter states, which may generically feature large logs that need to be resummed.

- For thermal wino, including full photon spectrum improves cross section sensitivity by ~50% - can be tested by current experiments, even with a large kpc-scale dark matter core in the Milky Way.

BONUS SLIDES

An aside

- From earlier: it is not sufficient to model energy resolution as counting photons in a bin of specified width

- If we modeled the spectrum as a line with intensity given by # photons in a bin - what would the bin width need to be to get the correct constraint (from full spectrum analysis)?

- Required bin width varies at the O(1) level as a function of DM mass

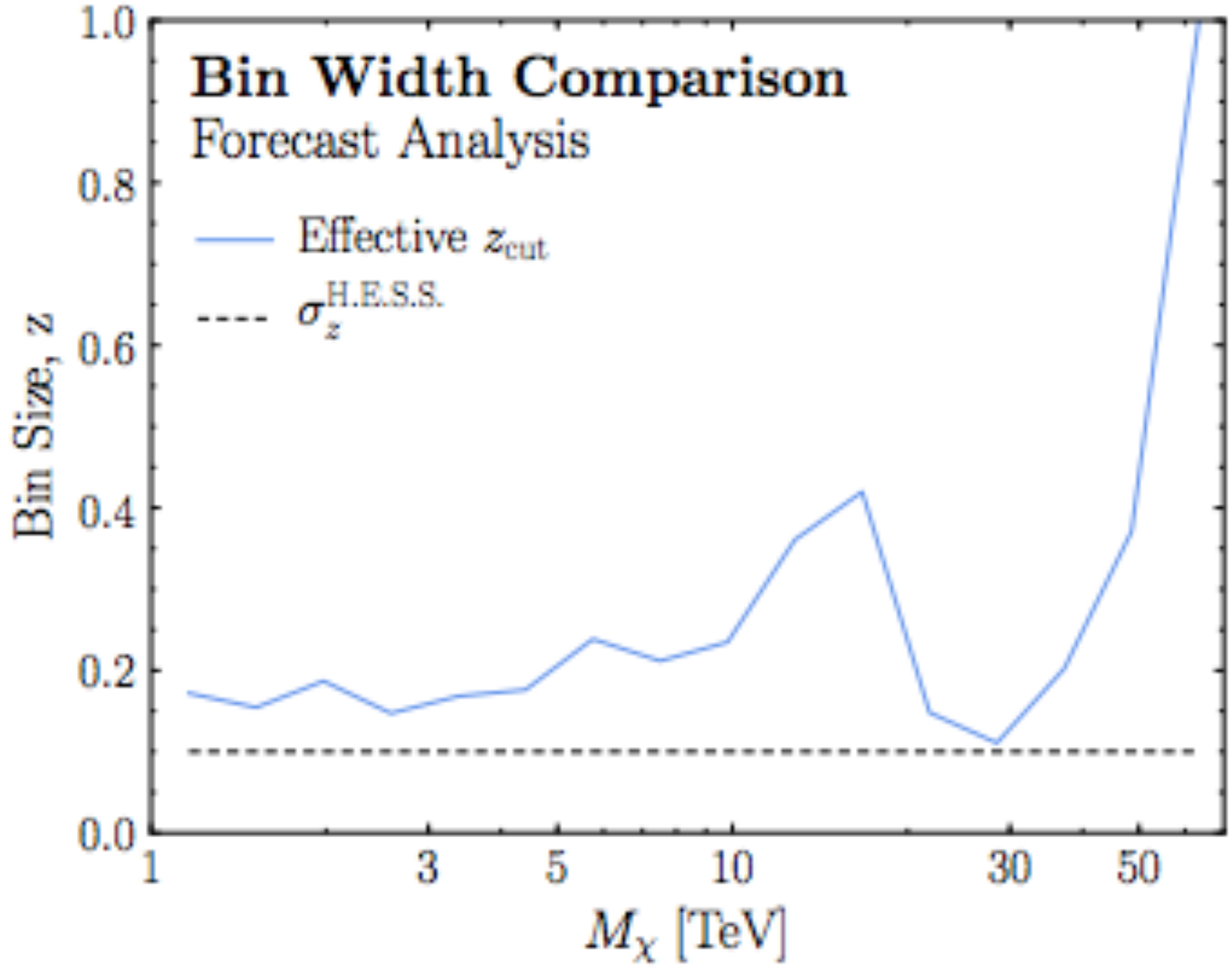

Rapidity renormalization

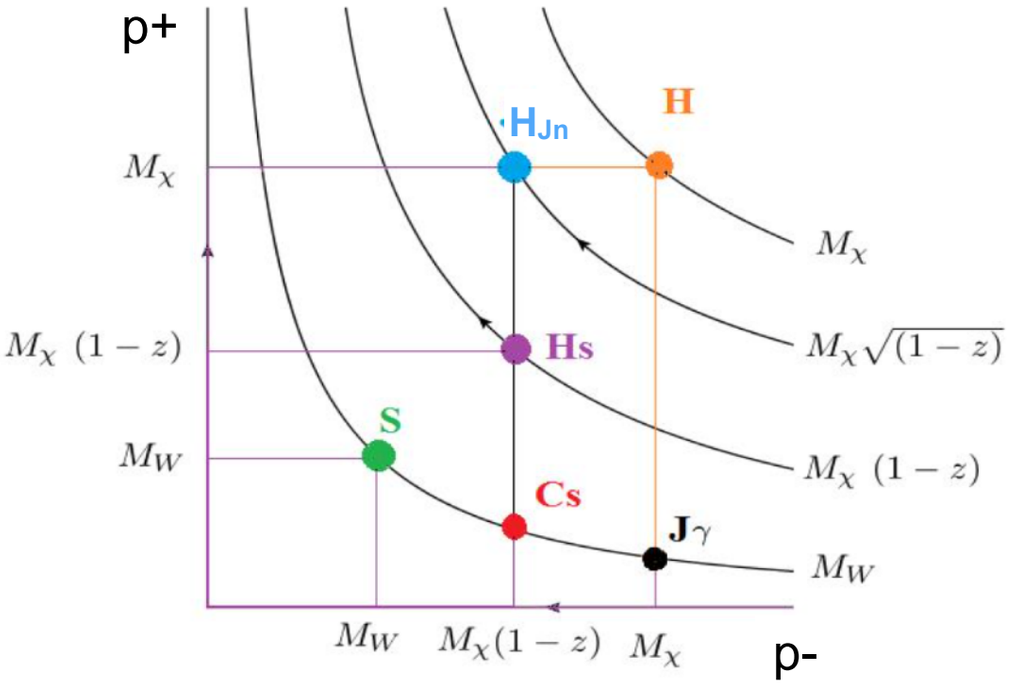

- "Virtuality" ~ $\sqrt{p^2}$ ~ Q λ for collinear and soft modes, Q λ^2 for ultrasoft modes - compare to usual regulating parameter μ appearing in RG evolution.
- But in $SCET_{II}$, collinear and soft modes have same virtuality / invariant mass - can be exchanged by a boost, distinguished only by their rapidity.
- Can't use running in virtuality to capture large logs between soft and collinear scales. Instead these logs arise from "rapidity divergences" - need to introduce "rapidity renormalization group" to resum them [Chiu et al '12].
- Introduce new (boost-violating) regularization parameter v.
- Natural scale of v (minimizing logs) is ~ Q for collinear modes, Q λ for soft modes, Q λ^2 for ultrasoft.
- Collinear-soft modes have natural scales $\mu \sim m_W$, $v \sim m_\chi(1-z)$.

RG evolution

anomalous dimensions

$$\gamma^H_{\mu,ij} = -2\,C_2\frac{\alpha_W}{\pi}\log\left(\frac{\mu^2}{(2\,M_\chi)^2\,z}\right)\delta_{ij}$$

$$\gamma_\mu^{H_{J_{\bar n}}} = 2\,C_2\frac{\alpha_W}{\pi}\log\left(\frac{\mu^2\,s}{2\,M_\chi}\right)$$

$$\frac{\mathrm{d}}{\mathrm{d}\log\mu}H_{S,11} = 0\,,\quad \frac{\mathrm{d}}{\mathrm{d}\log\mu}H_{S,ij} = \gamma^{H_S}_{\mu,jk}\,H_{S,ik}$$

$$\frac{\mathrm{d}}{\mathrm{d}\log\mu}H_{S,33} = -3\,C_2\frac{\alpha_W}{\pi}\log(\mu\,s)\,H_{S,33}\,,$$

$$\frac{\mathrm{d}}{\mathrm{d}\log\mu}H_{S,31} = 2\,C_2\frac{\alpha_W}{\pi}\log(\mu\,s)\,H_{S,33}\,,$$

$$\frac{\mathrm{d}}{\mathrm{d}\log\mu}H_{S,22} = -3\,C_2\frac{\alpha_W}{\pi}\log(\mu\,s)\,H_{S,22}\,,$$

$$\frac{\mathrm{d}}{\mathrm{d}\log\mu}H_{S,24} = C_2\frac{\alpha_W}{\pi}\log(\mu\,s)\,H_{S,22}\,.$$

evolution kernels

$$U_H\left(2M_\chi, m_W\right) = \exp\left(-2\,C_2\frac{\alpha_W}{\pi}\log^2\left(\frac{m_W}{2\,M_\chi}\right)\right)\,,$$

$$U_{H_{J_{\bar n}}}\left(\sqrt{2M_\chi/s}, m_W\right) = \exp\left(2\,C_2\frac{\alpha_W}{\pi}\log^2\left(m_W\sqrt{\frac{s}{2\,M_\chi}}\right)\right)\,,$$

$$H_{S,11}(m_W) = H_{S,11}(1/s)\,,$$

$$\begin{pmatrix} H_{S,33}(m_W) \\ H_{S,31}(m_W)\end{pmatrix} = \begin{pmatrix} U_{H_S} & 0 \\ 2\,(1-U_{H_S})/3 & 1\end{pmatrix}\begin{pmatrix} H_{S,33}(1/s) \\ H_{S,31}(1/s)\end{pmatrix}\,,$$

$$\begin{pmatrix} H_{S,22}(m_W) \\ H_{S,24}(m_W)\end{pmatrix} = \begin{pmatrix} U_{H_S} & 0 \\ (1-U_{H_S})/3 & 1\end{pmatrix}\begin{pmatrix} H_{S,22}(1/s) \\ H_{S,24}(1/s)\end{pmatrix}\,,$$

$$U_{H_S} = \exp\left(-\frac{3}{2}\,C_2\frac{\alpha_W}{\pi}\log^2\left(m_W\,s\right)\right)$$

Limiting cases

Plus functions defined by: $$\int_0^\infty dq \left(\frac{\ln\left(\frac{q}{U}\right)}{q}\right)_+ F(q) = \int_U^\infty dq \left(\frac{\ln\left(\frac{q}{U}\right)}{q}\right) F(q)$$

$\mathcal{L}_1^S$ cuts off for $z > 1 - \dfrac{m_W}{2m_\chi}$

$\mathcal{L}_1^J$ cuts off for $z > 1 - \left(\dfrac{m_W}{2m_\chi}\right)^2$

separation between line and continuum regimes

Thus if we integrate from $z = 1 - \left(\dfrac{m_W}{2m_\chi}\right)^2$ to 1, only the line contributes:

$$\frac{\mathrm{d}\sigma}{\mathrm{d}z} = 4\,|s_{0\pm}|^2\,\sigma^{\text{tree}}\; e^{-2\,\Gamma_0\,\tilde{\alpha}_W\,L_\chi^2}\;\delta(1-z)$$

matches exclusive result from Ovanesyan et al ’15, Cohen et al ‘15

If we integrate from 0 to 1, we recover the semi-inclusive result:

$$\int_0^1 dz \frac{d\sigma}{dz} = \frac{\pi\alpha_W^2 \sin^2\theta_W}{2M_\chi^2 v}\left\{\frac{4}{3}|s_{00}|^2 f_- + 2|s_{0\pm}|^2 f_+ + \frac{2\sqrt{2}}{3}\left(s_{00}s_{0\pm}^* + c.c\right) f_-\right\}$$

$$f_\pm = 1 \pm e^{-\frac{3}{2}\Gamma_0\tilde{\alpha}_W L_\chi^2}$$

matches Baumgart et al ‘15

- Gauge invariant gauge boson operator: $\mathcal{B}_n^\mu(x) = \frac{1}{g}\left[W_n^\dagger(x)\, iD_{n\perp}^\mu W_n(x)\right]$
- Collinear Wilson line: $W_n = \left[\sum_{\text{perms}} \exp\left(-\frac{g}{\bar{n}\cdot\mathcal{P}}\bar{n}\cdot A_n(x)\right)\right]$
- Ultrasoft Wilson line: $Y_n^{(r)}(x) = \mathbf{P}\exp\left[ig\int_0^0 \mathrm{d}s\, n\cdot A_{us}^a(x+sn)T_{(r)}^a\right]$
- Soft Wilson line: $S_n^{(r)}(x) = \mathbf{P}\exp\left[ig\int_{-\infty}^0 \mathrm{d}s\, n\cdot A_s^a(x+sn)T_{(r)}^a\right]$

- Collinear-soft Wilson lines:

$$X_n^{(r)}(x) = \mathbf{P}\exp\left[ig\int_{-\infty}^0 \mathrm{d}s\, n\cdot A_{cs}^a(x+sn)T_{(r)}^a\right] \qquad V_n^{(r)}(x) = \mathbf{P}\exp\left[ig\int_{-\infty}^0 \mathrm{d}s\, \bar{n}\cdot A_{cs}^a(x+s\bar{n})T_{(r)}^a\right]$$

- Hard Lagrangian / hard function:

$$\mathcal{L}_{\text{hard}}^{(0)} = \sum_{r=1}^{2} C_r(M_\chi,\mu)\left(\chi_v^{aT}\, i\sigma_2\, \chi_v^b\right)\left(Y_r^{abcd}\,\mathcal{B}_{n\perp}^{ic}\,\mathcal{B}_{\bar{n}\perp}^{jd}\right) i\,\epsilon^{ijk}(n-\bar{n})^k \qquad H_{ij} = C_i C_j$$

$$Y_1^{abcd} = \delta^{ab}\left(Y_n^{ce}S_{\bar{n}}^{de}\right), \qquad Y_2^{abcd} = \left(Y_v^{ae}Y_n^{ce}\right)\left(Y_v^{bf}Y_{\bar{n}}^{df}\right) \qquad C_1(\mu) = -C_2(\mu) = -\pi\,\frac{\alpha_2(\mu)}{M_\chi}$$

- Rapidity regulators:

$$S_n = \left[\sum_{\text{perms}} \exp\left(-\frac{g}{n\cdot\mathcal{P}} \frac{\omega\,|2\,\mathcal{P}^z|^{-\eta/2}}{\nu^{-\eta/2}} n\cdot A_s(x) \right) \right],$$

$$W_{\bar{n}} = \left[\sum_{\text{perms}} \exp\left(-\frac{g}{n\cdot\mathcal{P}} \frac{\omega^2\,|n\cdot\mathcal{P}|^{-\eta/2}}{\nu^{-\eta/2}} n\cdot A_{\bar{n}}(x) \right) \right],$$

- Soft/collinear measurement operators:

$$\widehat{\mathcal{M}}_s|X_s\rangle = \frac{2}{4\,M_\chi} \sum_{i\in X_s} n\cdot p_i |X_s\rangle\,, \qquad \widehat{\mathcal{M}}_c|X_c\rangle = \frac{1}{4\,M_\chi^2} \left(\sum_{i\in X_c} p_i^\mu \right)^2 |X_c\rangle \qquad \widehat{\mathcal{M}}_{cS}|X_{cS}\rangle = \frac{2}{4\,M_\chi} \sum_{i\in X_{cS}} \bar{n}\cdot p_i |X_{cS}\rangle$$

- Soft functions: $S'_{ij}(1-z_s, m_W) = \left\langle 0 \middle| \bar{\mathrm{T}}\, Y_i^\dagger(0)\; \delta\Big((1-z_s) - \widehat{\mathcal{M}}_s\Big)\, \mathrm{T}\, Y_j(0) \middle| 0 \right\rangle$

- Collinear/soft function: $\tilde{S}_j^{aba'b'} = (C_S S)_j^{aba'b'}$

$$C_S\big(M_\chi, 1-z_c, m_W, \mu, \nu\big) = \left\langle 0 \middle| (X_n V_n)^\dagger \delta\Big((1-z_c) - \widehat{M}_{cS}\Big) X_n V_n \middle| 0 \right\rangle$$

$$\tilde{S}_1^{aba'b'} = \left\langle 0 \middle| \left(Y_n^{3f'} Y_{\bar{n}}^{dg'}\right)^\dagger \delta\Big((1-z_s) - \widehat{M}_{C_S}\Big) \left(Y_n^{3f} Y_{\bar{n}}^{dg}\right) \middle| 0 \right\rangle \delta^{f'g'}\delta^{a'b'}\delta^{fg}\delta^{ab}\,,$$

$$\tilde{S}_2^{aba'b'} = \left\langle 0 \middle| \left(Y_n^{ce} Y_{\bar{n}}^{Ae}\right)^\dagger \delta\Big((1-z_s) - \widehat{M}_{cS}\Big) Y_n^{c'g'} Y_{\bar{n}}^{A'g'} \middle| 0 \right\rangle \left\langle 0 \middle| \left[S_n^{3c} S_n^{3c'} S_v^{a'A'} S_v^{aA}\right] \middle| 0 \right\rangle \delta^{bb'}\,,$$

$$\tilde{S}_3^{aba'b'} = \left\langle 0 \middle| \left(Y_n^{ce} Y_{\bar{n}}^{B'e}\right)^\dagger \delta\Big((1-z_s) - \widehat{M}_{cS}\Big) Y_n^{c'g'} Y_{\bar{n}}^{A'g'} \middle| 0 \right\rangle$$
$$\times \left(\left\langle 0 \middle| \left[S_n^{3c} S_n^{3c'} S_v^{a'A'} S_v^{b'B'}\right] \middle| 0 \right\rangle \delta^{ab} + \left\langle 0 \middle| \left[S_n^{3c} S_n^{3c'} S_v^{aA'} S_v^{bB'}\right] \middle| 0 \right\rangle \delta^{a'b'} \right). \qquad (4.28)$$

Tree-level functions

hard and hard-soft functions

$$H_{11} = 1, \quad H_{22} = 1, \quad H_{12} = H_{21} = -1$$

$$H_{S,11} = 1, \quad H_{S,22} = 2, \quad H_{S,33} = 1$$

combined collinear-soft + soft function $\tilde{S}_j^{aba'b'} = (C_S S)_j^{aba'b'}$

$$\tilde{S}_1^{aba'b'} = \delta^{a'b'}\delta^{ab}\,, \qquad \tilde{S}_2^{aba'b'} = \delta^{a3}\delta^{a'3}\delta^{bb'}\,,$$

$$\tilde{S}_3^{aba'b'} = \delta^{a3}\delta^{b3}\delta^{a'b'} + \delta^{a'3}\delta^{b'3}\delta^{ab}\,, \qquad \tilde{S}_4^{aba'b'} = \delta^{a'a}\delta^{bb'}\,.$$

- Jet functions:

$$J'^{\,dd'}_{\bar{n}}\left(M_\chi, 1-z_c, m_W\right) = \left\langle 0\middle| B^{d'}_{\bar{n}\perp}\,\delta\Big((1-z_c)-\widehat{\mathcal{M}}_c\Big)\delta\big(M_\chi-\bar{n}\cdot\mathcal{P}\big)\,\delta^2\big(\vec{\mathcal{P}}_\perp\big)\,B^{d}_{\bar{n}\perp}\middle|0\right\rangle$$

$$J_\gamma(m_W) = \left\langle 0\middle| B^{c}_{n\perp}\middle|\gamma\right\rangle\left\langle\gamma\middle| B^{c}_{n\perp}\middle|0\right\rangle,$$

- Recoiling jet function:

$$J_{\bar{n}}(k) = \delta(2M_\chi k^+) + \frac{\alpha_W}{4\pi}\left(\frac{4C_2(G)\log(2M_\chi k^+/\mu^2)-\beta_0}{2M_\chi k^+}\right)_+$$

- Photon jet function:

$$J^{(0)}_{\bar{n}} = -2\,,$$

$$J^{(1)}_{\bar{n}} = -2C_2\frac{\alpha_W}{\pi}\left(\frac{\mu}{M}\right)^{2\epsilon}\left(\frac{\nu}{2E_\gamma}\right)^{\eta}\frac{\Gamma(\epsilon)}{\eta} + \frac{\alpha_W}{2\pi}\Gamma(\epsilon)\left(\frac{\mu}{M}\right)^{2\epsilon}\left[\frac{11}{3}C_2-\frac{4}{3}n_f C(R)\right]$$

Beyond LL: high-scale matching

- At NLL, only tree-level high-scale matching is needed. For NLL', we have performed it at one-loop.

- Compute (25) one-loop diagrams in the full theory, match onto $SCET_{EW}$ operators. We provide analytic expressions graph-by-graph [appendix A of Ovanesyan, Rodd, TRS & Stewart '16].

$$C_1(\mu) = -\frac{\pi\alpha_2(\mu)}{m_\chi} + \frac{\alpha_2(\mu)^2}{4m_\chi}\left[2\ln^2\frac{\mu^2}{4m_\chi^2}\right.$$
$$\left.+2\ln\frac{\mu^2}{4m_\chi^2} + 2i\pi\ln\frac{\mu^2}{4m_\chi^2} + 8 - \frac{11\pi^2}{6}\right],$$
$$C_2(\mu) = \frac{\pi\alpha_2(\mu)}{m_\chi} - \frac{\alpha_2(\mu)^2}{2m_\chi}\left[\ln^2\frac{\mu^2}{4m_\chi^2}\right.$$
$$\left.+3\ln\frac{\mu^2}{4m_\chi^2} - i\pi\ln\frac{\mu^2}{4m_\chi^2} - \frac{5\pi^2}{12}\right].$$

example diagrams

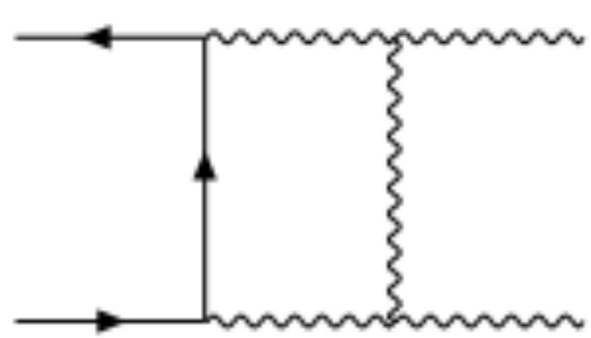

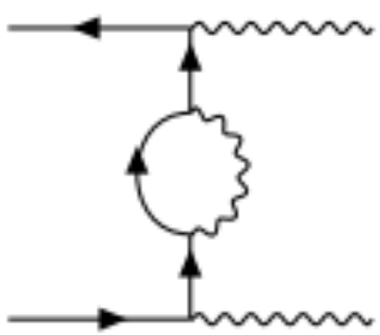

High-scale matching diagrams

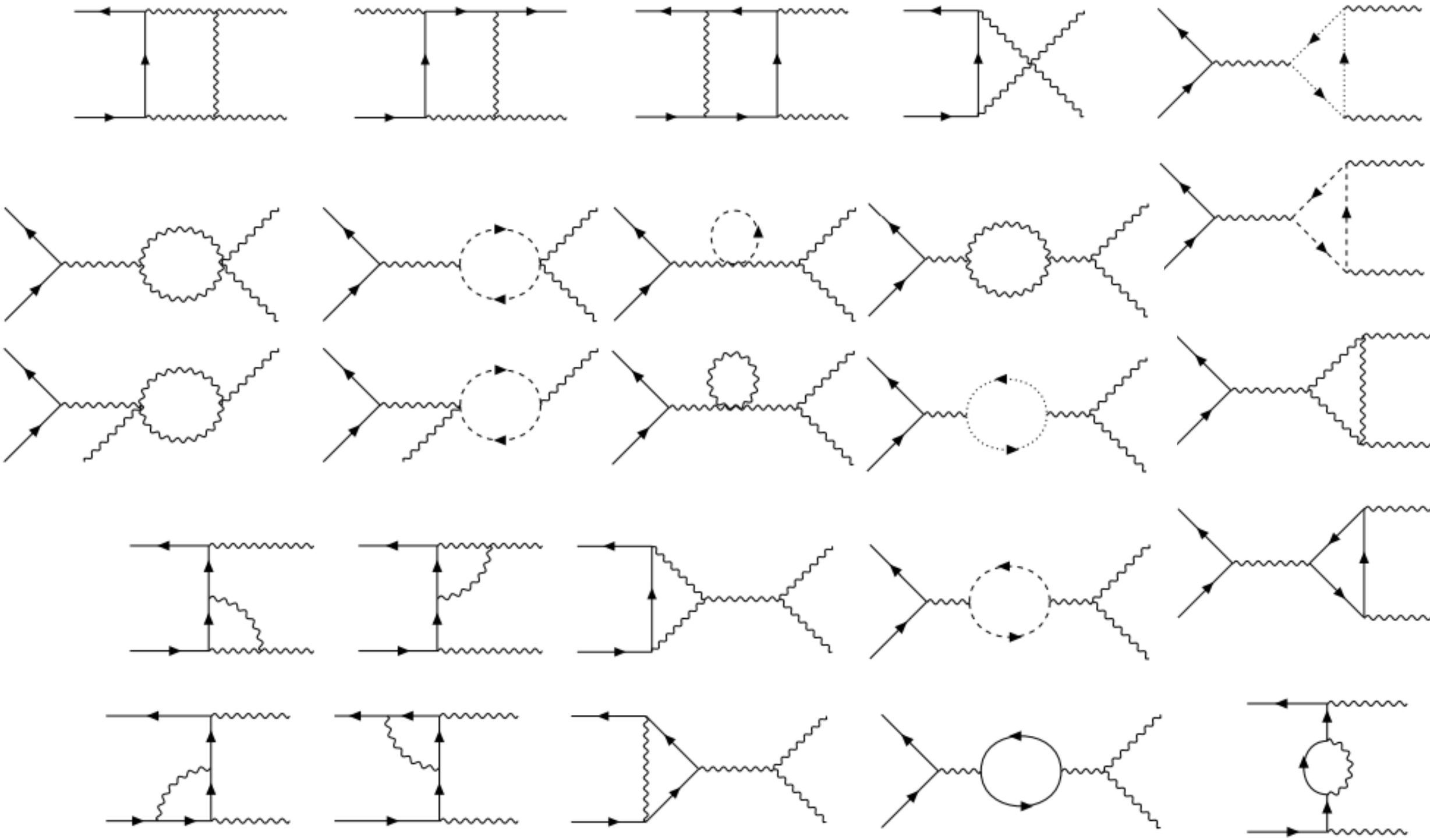

Beyond LL: low-scale matching

- At NLL, only tree-level low-scale matching + log piece of one-loop matching is needed. For NLL', we have performed the full matching at one-loop.

- Compute one-loop diagrams that appear in $SCET_{EW}$ but not $SCET_{\gamma}$, match onto $SCET_{\gamma}$ operators after electroweak symmetry breaking.

$$\exp\left[\hat{D}^X(\mu)\right] = \left[\hat{D}_s(\mu)\right]\left[D_c^X(\mu)\mathbb{I}\right]\exp\left[\sum_{i\in X} D_c^i(\mu)\mathbb{I}\right]$$

X labels final state γγ, γZ, ZZ

non-diagonal matrix from soft interactions

initial state diagonal contribution

final state diagonal contribution

$$\hat{D}_s = \begin{pmatrix} 1+\frac{\alpha_2(\mu)}{2\pi}\left[\ln\frac{m_W^2}{\mu^2}(1-2i\pi)+c_W^2\ln\frac{m_Z^2}{\mu^2}\right] & \frac{\alpha_2(\mu)}{2\pi}\ln\frac{m_W^2}{\mu^2}(1-i\pi) \\ 1+\frac{\alpha_2(\mu)}{2\pi}\ln\frac{m_W^2}{\mu^2}(2-2i\pi) & 1 \end{pmatrix}$$

$$D_c^X(\mu) = 1-\frac{\alpha_2(\mu)}{2\pi}\left[\ln\frac{m_W^2}{\mu^2}+c_W^2\ln\frac{m_Z^2}{\mu^2}\right]$$

contribution needed for NLL

$$D_c^i(\mu) = \frac{\alpha_2(\mu)}{2\pi}\left[\ln\frac{m_W^2}{\mu^2}\ln\frac{4m_\chi^2}{\mu^2}-\frac{1}{2}\ln^2\frac{m_W^2}{\mu^2}\right.$$

finite constants dependent on final state

$$\left.-\ln\frac{m_W^2}{\mu^2}+c_1^i\ln\frac{m_Z^2}{\mu^2}+c_2^i\right]$$

Low-scale matching diagrams

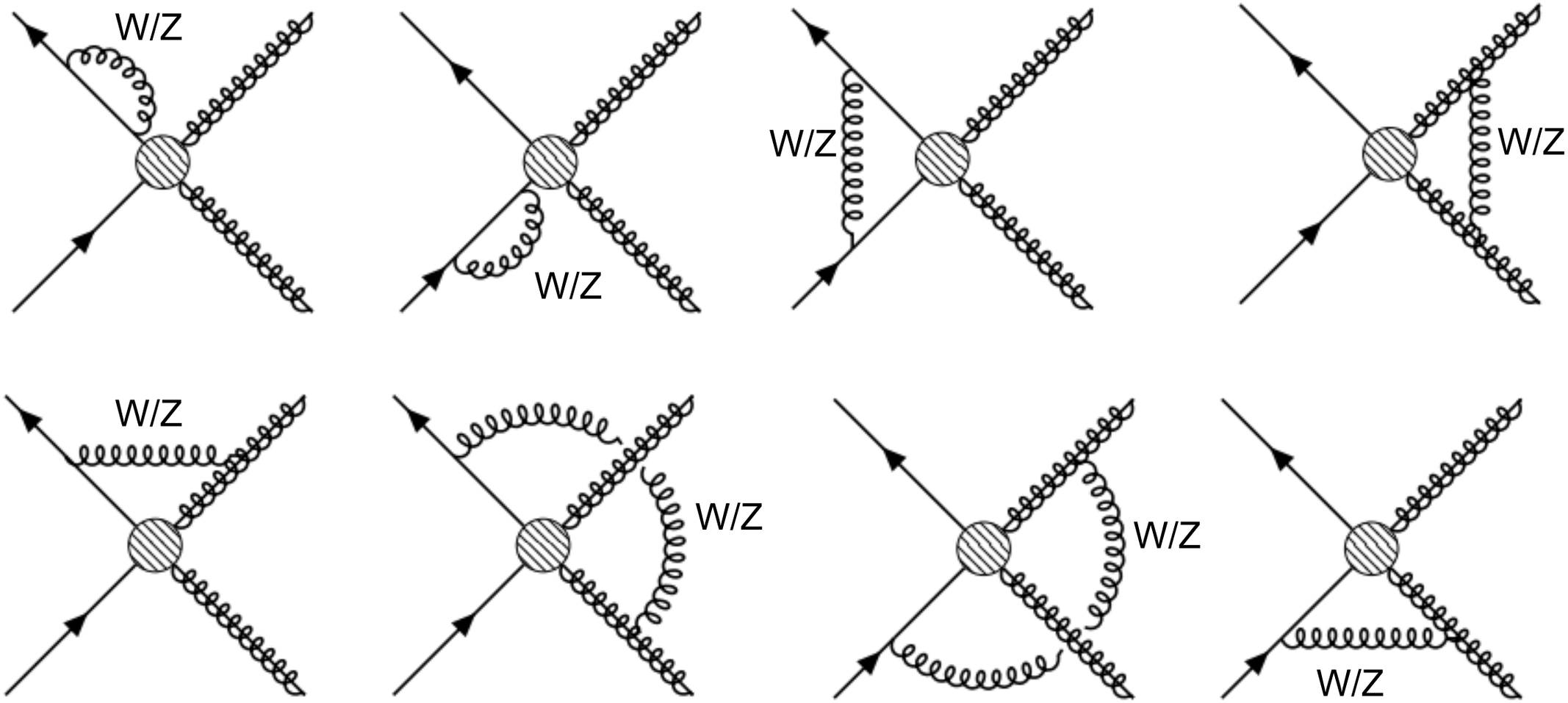

Beyond LL: the anomalous dimension

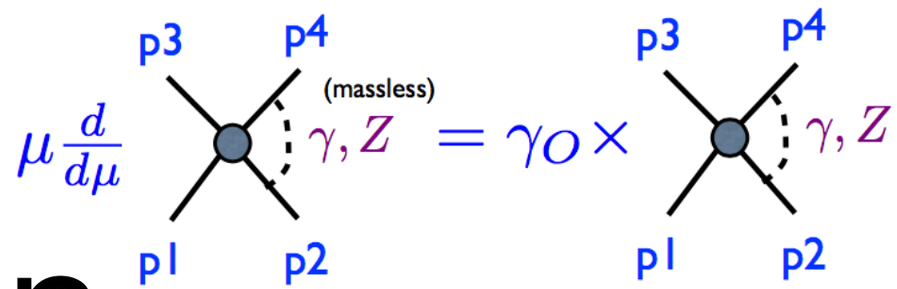

- Novel feature of this case: incoming particles are non-relativistic, momentum 4-vectors in same direction v = (1,0,0,0). Gives rise to soft S_v Wilson lines that can interact with each other or themselves.

- Anomalous dimension has two contributions:
  - Collinear piece, must be calculated to 2-loop for NLL, but is unchanged from case with lightlike incoming particles - can use results in literature [Chiu et al '09].
  - Soft piece - needs to be recalculated, but only at one-loop [Ovanesyan, TRS & Stewart '15].

$$\hat{\gamma} = 2\gamma_{W_T}\mathbb{I} + \hat{\gamma}_S \qquad \Gamma_1^g = 8\left(\tfrac{70}{9} - \tfrac{2}{3}\pi^2\right)$$

$$\gamma_{W_T} = \frac{\alpha_2}{4\pi}\Gamma_0^g \ln\frac{2m_\chi}{\mu} - \frac{\alpha_2}{4\pi}b_0 + \left(\frac{\alpha_2}{4\pi}\right)^2 \Gamma_1^g \ln\frac{2m_\chi}{\mu}$$

$$\hat{\gamma}_S^{\rm NLL} = \frac{\alpha_2}{\pi}(1 - i\pi)\begin{pmatrix} 2 & 1 \\ 0 & -1 \end{pmatrix} - \frac{2\alpha_2}{\pi}\begin{pmatrix} 1 & 0 \\ 0 & 1 \end{pmatrix}$$

Diagrams for soft anom. dim.

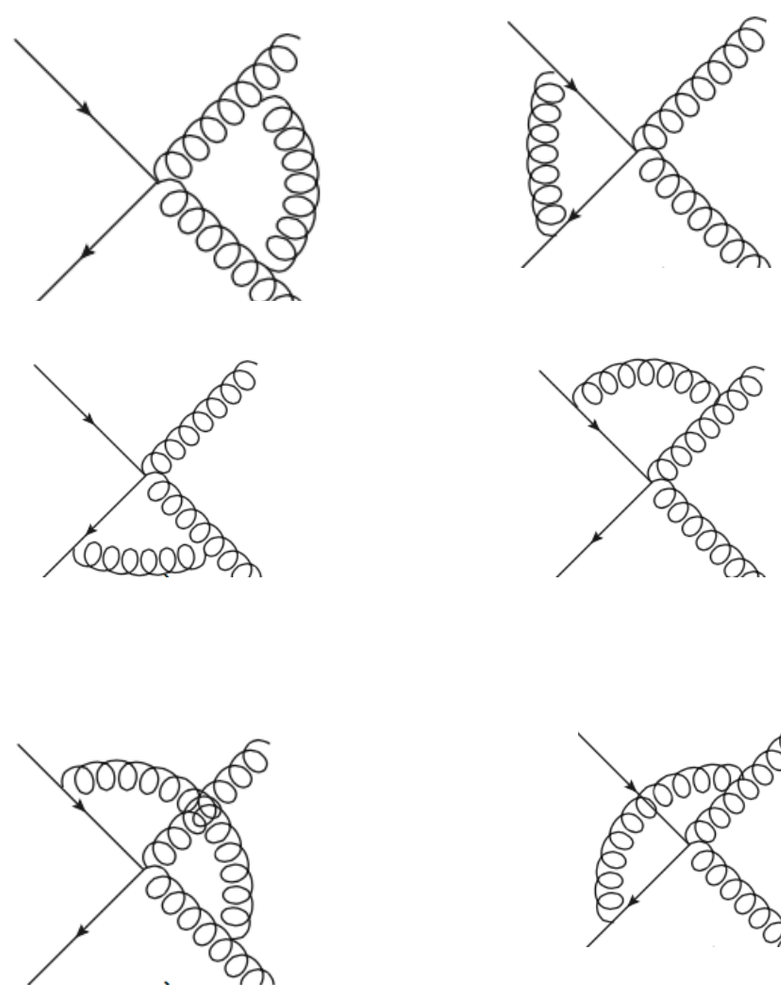

+wavefunction renormalization

The dark matter density profile

- Limits on flux should always be understood as joint limits on DM model + DM density profile.

- Thermal wino naively appears ruled out - but could still be viable if DM density in inner Galaxy is smaller than assumed.

$z = 0$	$r_{\rm core}$ (kpc)	$r_{\rm core}/R_{\rm vir}$
m09	0.17	0.0048
m10	0.38	0.0073
m11	4.7	0.034
m12v	1.4	0.0061
m12i	2.0	0.0073
m12q	1.2	0.0043
m10h1297	2.0	0.032
m10h1146	2.1	0.033
m10h573	3.6	0.041
m11h383	5.7	0.041

- Usually limits are expressed in terms of Einasto/NFW density profiles - rise steeply toward Galactic Center.

- Simulations suggest flattened cores of O(1 kpc) size may be possible in Milky-Way-sized galaxies [e.g. Chan et al MNRAS 524 ‘15].

- Measurements of DM in the Galactic bulge suggest classic NFW profiles should have ≲ 2 kpc cores [Hooper PDU15 ’17].

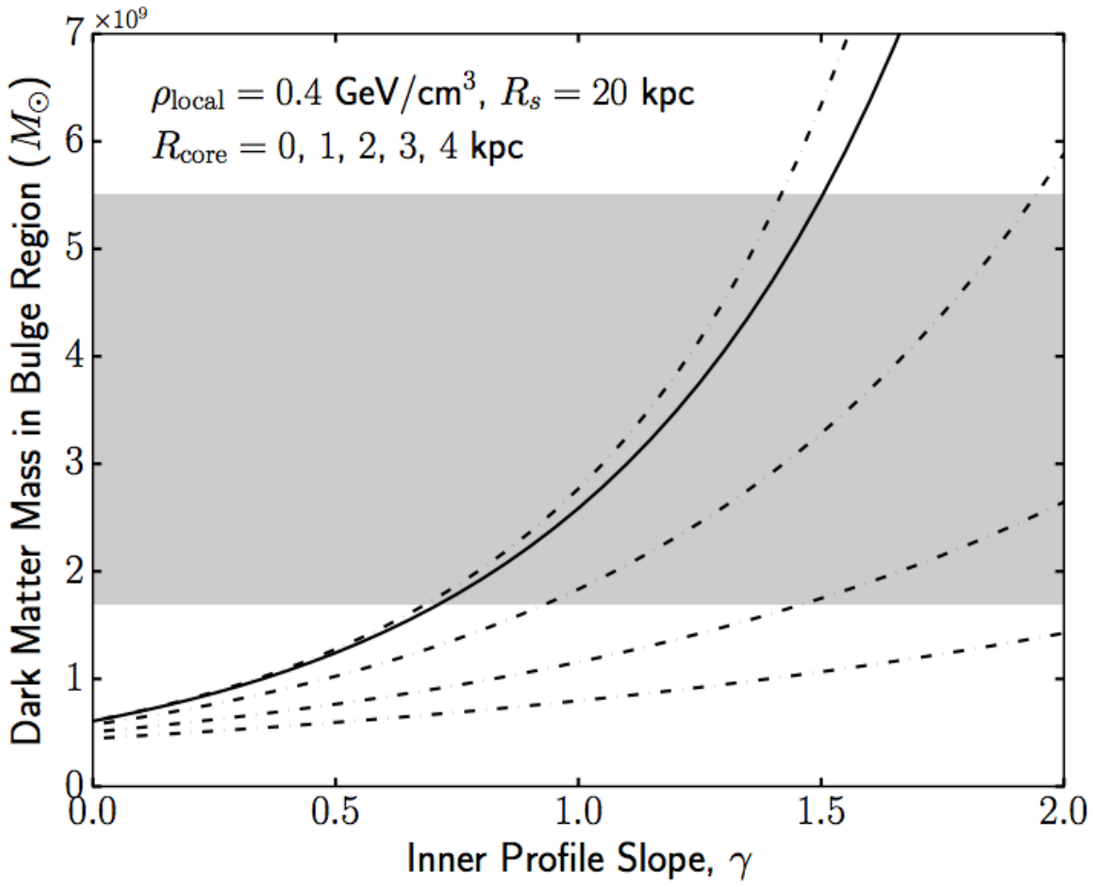

The dark matter density profile

- Limits on flux should always be understood as joint limits on DM model + DM density profile.
- Thermal wino naively appears ruled out - but could still be viable if DM density in inner Galaxy is smaller than assumed.

$z = 0$	$r_{\rm core}$ (kpc)	$r_{\rm core}/R_{\rm vir}$
m09	0.17	0.0048
m10	0.38	0.0073
m11	4.7	0.034
m12v	1.4	0.0061
m12i	2.0	0.0073
m12q	1.2	0.0043
m10h1297	2.0	0.032
m10h1146	2.1	0.033
m10h573	3.6	0.041
m11h383	5.7	0.041

- Usually limits are expressed in terms of Einasto/NFW density profiles - rise steeply toward Galactic Center.
- Simu
- Measurem
suggest classic NFW profiles should have ≲ 2 kpc cores [Hooper PDU15 ’17].

can we constrain the “thermal wino + 1-2 kpc core” scenario?

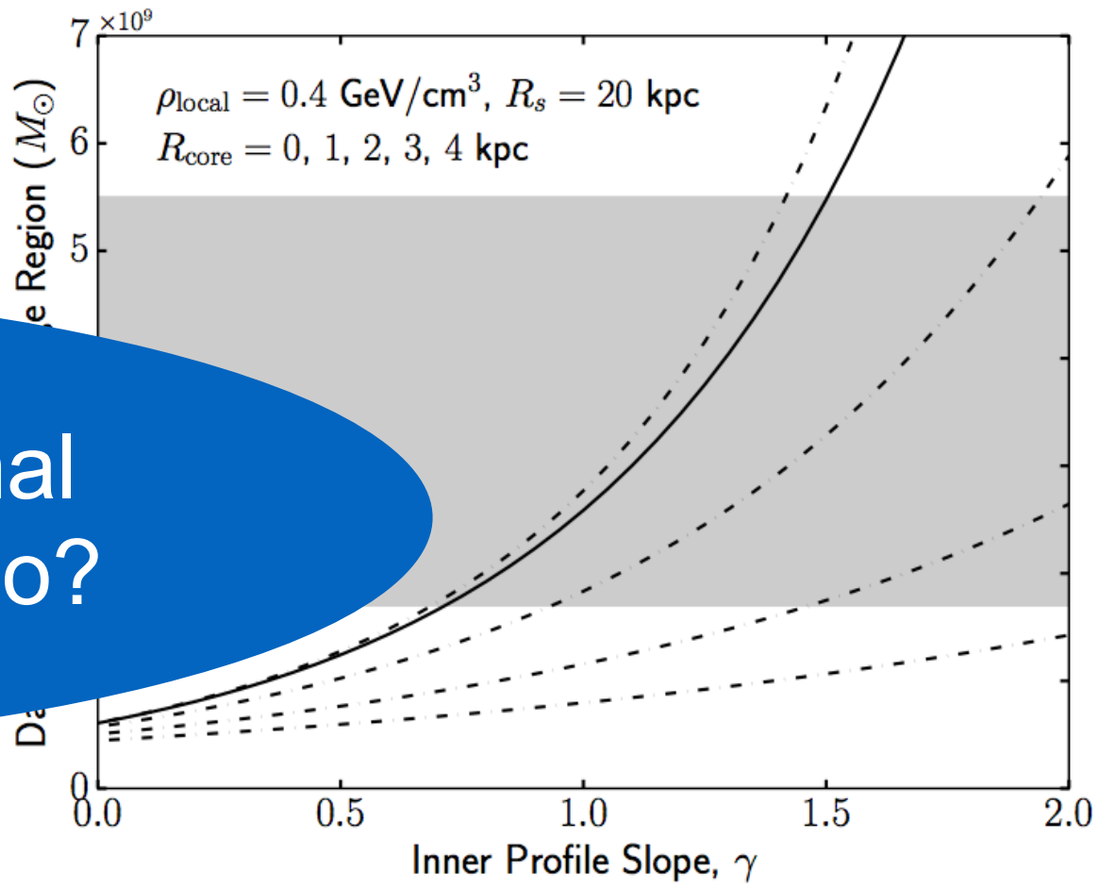

The analysis

- 2D binned likelihood analysis in position (ROI #) and energy, to exploit knowledge of DM spectrum/distribution.

- Spatial bins are concentric rings, 0.1 degrees wide (masked areas removed).

- Default analysis is within 1 degree radius of GC: 7 Regions of Interest (ROIs), as region within 0.3 degrees of plane is masked.

- Also consider observations with up to 4 degree radius (37 ROIs total).

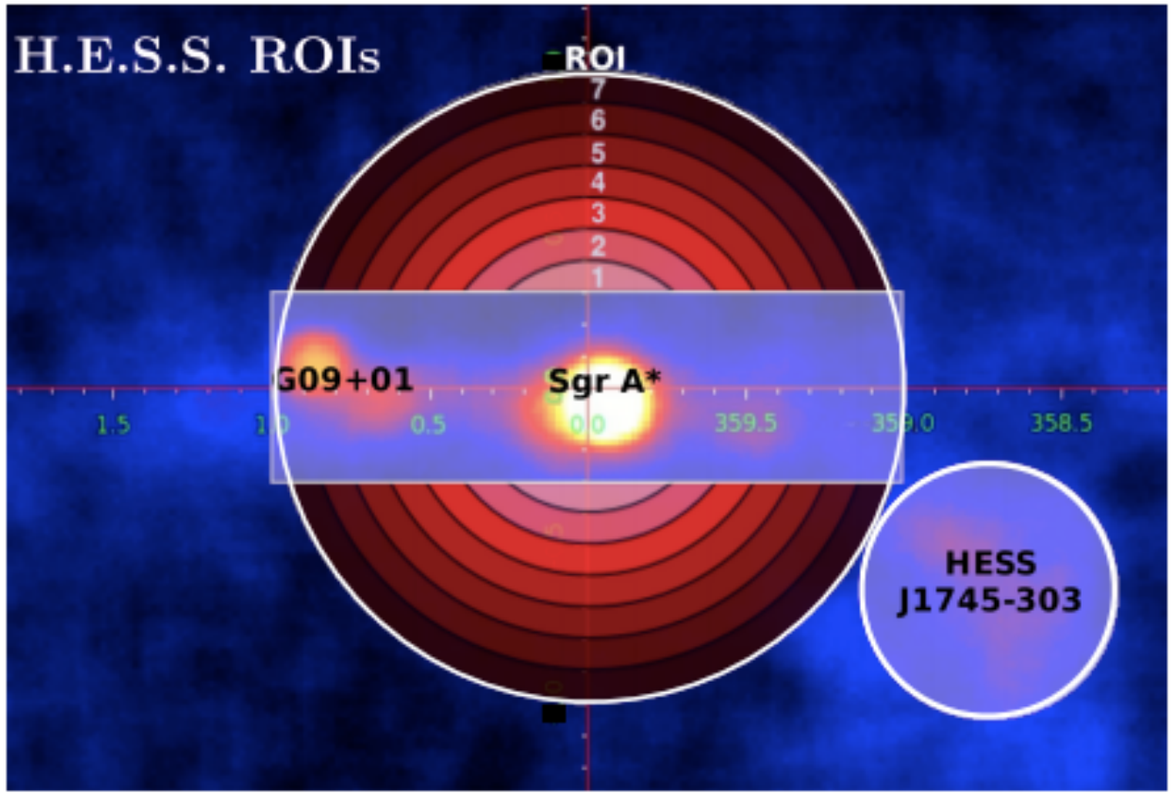

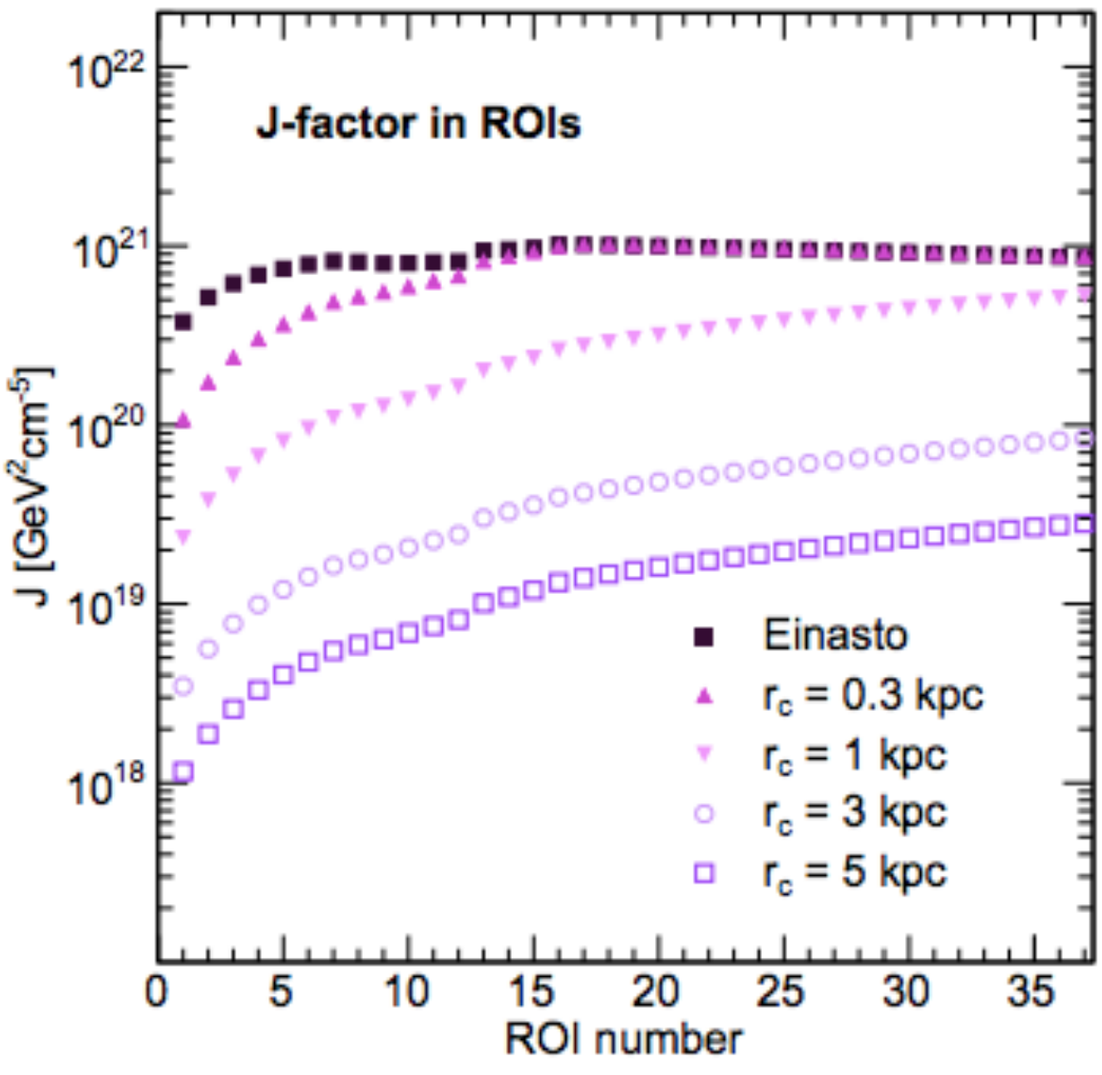

The need for resummation

- Hryczuk & Iengo ’12 studied inclusion of non-ladder loop diagrams in hard amplitudes A^0.

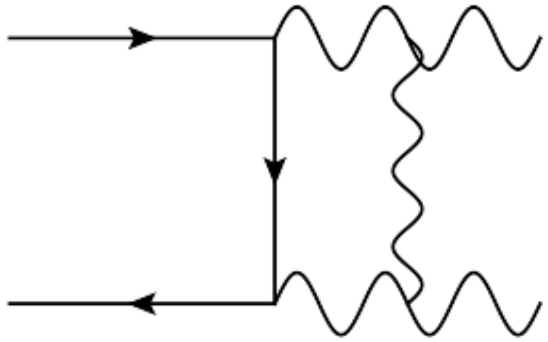

- Found surprisingly large suppression, e.g. ~40% in amplitude for 3 TeV wino, leading to factor-of-3 difference in cross section.

- Suggests breakdown of perturbative expansion.

- Turns out to arise from large $\log^2(m_{DM}/m_W)$ terms.

- Large loop corrections - also large contributions to real photon emission.

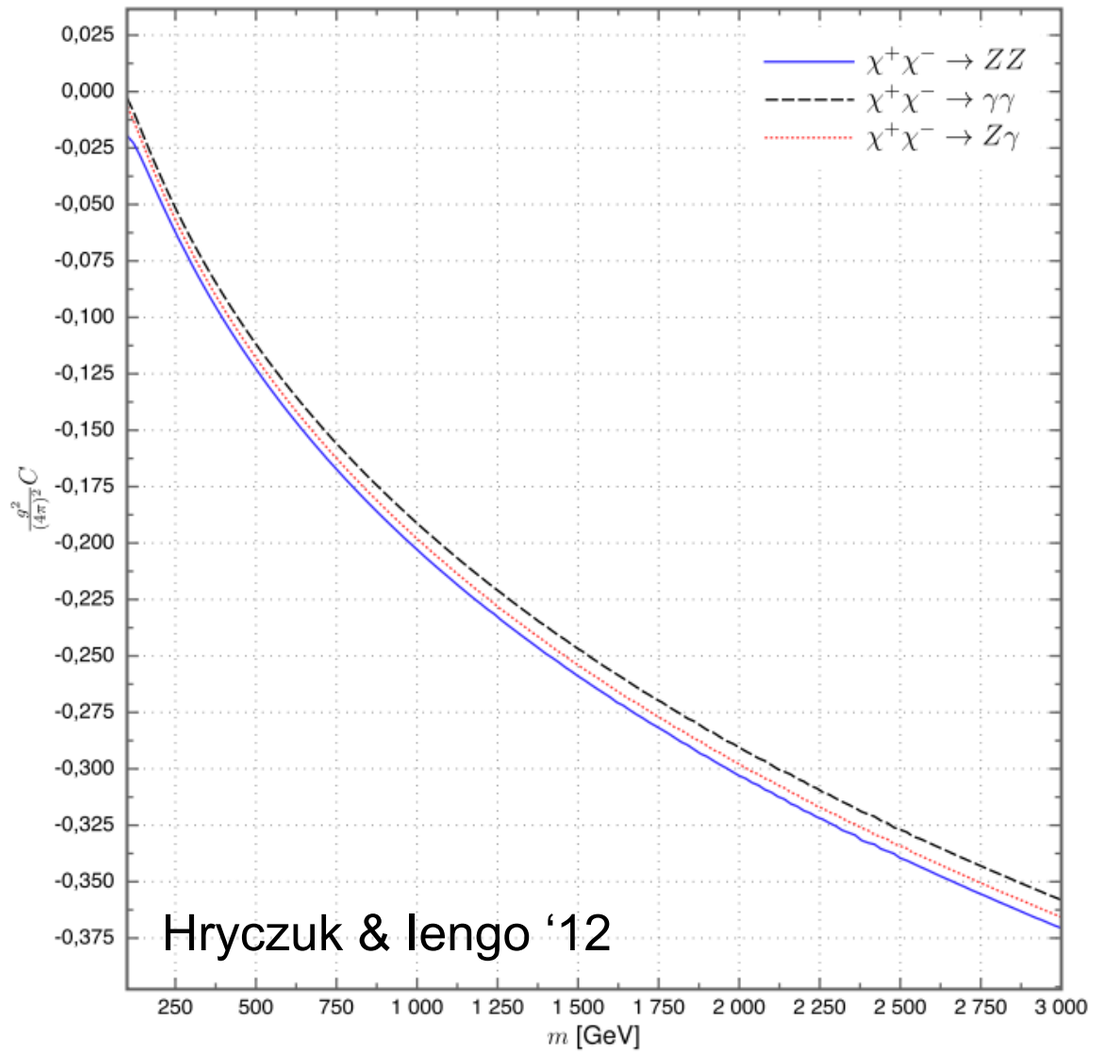

The line cross section

Ovanesyan, TRS et al PRL 114, 211302 ‘15 & PRD 95, 055001 ’17; see also Cohen et al ‘15

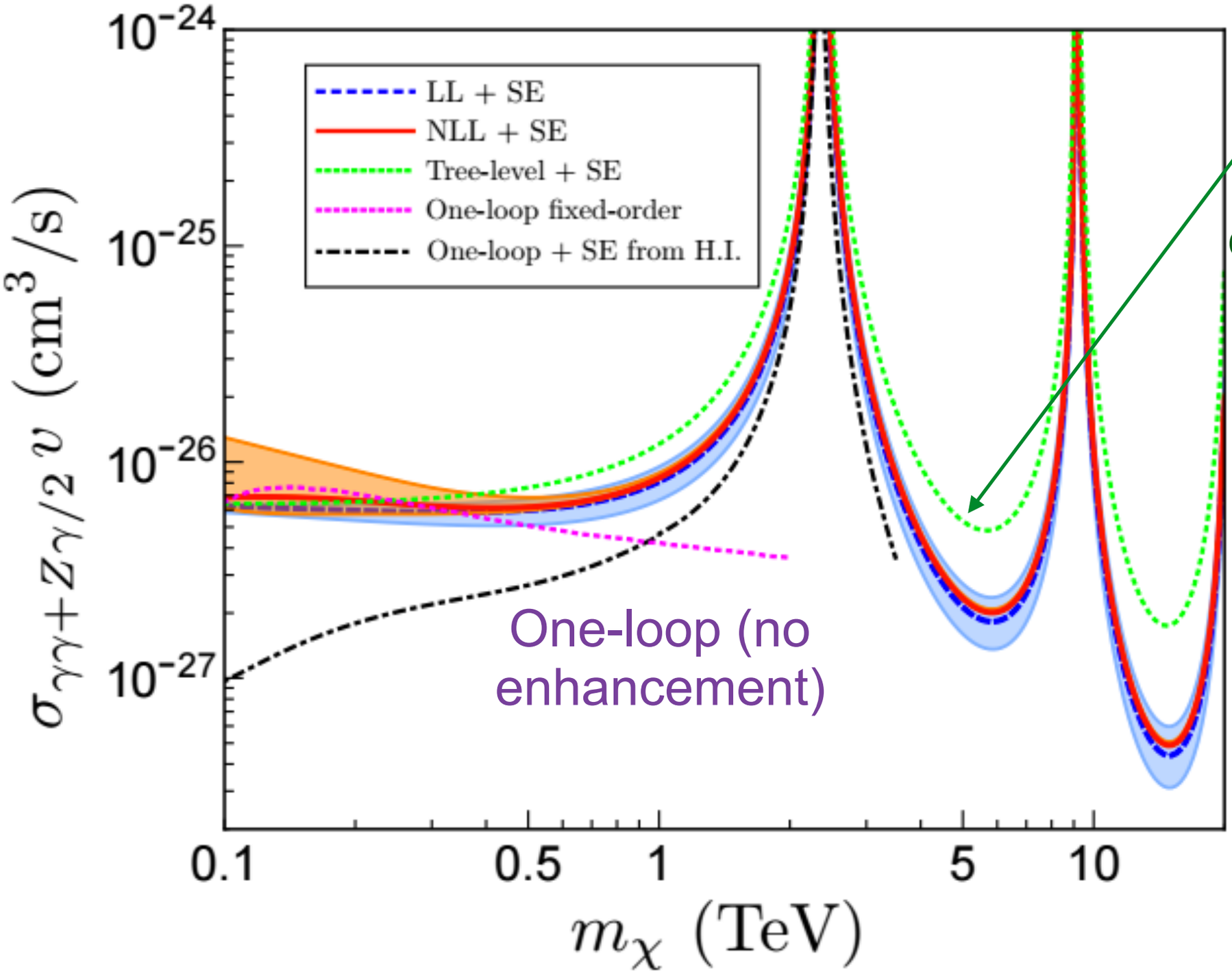

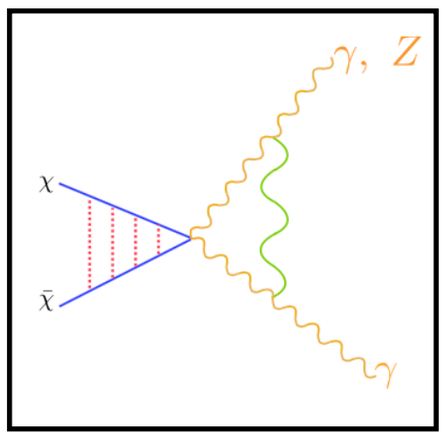

The line cross section

Ovanesyan, TRS et al PRL 114, 211302 ‘15 & PRD 95, 055001 ’17; see also Cohen et al ‘15